The increase in the total cross sections for hadronic interactions with increasing energy

E. M. Levin and M. G. Ryskin

B. P. Konstantinov Leningrad Institute of Nuclear Physics, Academy of Sciences of the USSR
Usp. Fiz. Nauk **158**, 178–214 (June 1989)

The reasons for an increase in the cross sections and the range of interaction of hadrons with increasing energy are discussed. A picture of fast hadron collisions that enables one to explain on the basis of quantum chromodynamics perturbation theory the main qualitative features of present-day experimental data is examined.

1. INTRODUCTION

The new generation accelerators that are now becoming operational will be used to investigate the interaction between elementary particles at energies that were previously considered to be in the realm of science fiction. The first of these is the proton-antiproton collider at CERN (Sp$\bar{p}$S). It is already operation and covers the center of mass energy range 200–900 GeV. The second collider is at FNAL. Its energy is twice as high: $s^{1/2} = 1.8$ TeV (900×900 (GeV). The 6-TeV accelerating and storing system UNK is being built in the Soviet Union, and a 40-TeV superconducting supercollider (SSC) is being planned in the USA. As preparation for the routine use of these accelerators, it will be useful to summarize modern ideas on the old and traditional problem in high-energy physics, i.e., the energy dependence of the total cross section σ_t for the hadron-hadron interactions and, most importantly, the nature of the typical (and not rare) processes responsible for the interaction. This is indeed the aim of the present review.

We shall confine our attention to the most important inelastic and, to a lesser extent, diffraction processes with relatively high cross sections. Rare events involving the production of intermediate bosons (W,Z), new heavy particles, and jets with high transverse momenta q_t that remove an appreciable fraction x of the initial-hadron energy, e.g., $S^{1/2} = 500$ GeV in the case of the Sp$\bar{p}$S collider and $q_t > 30$ GeV in the case of jets, will not be considered in this review. Elastic cross sections for $|t| > 1$–2 GeV^2, for which $d\sigma/dt$ is lower by a factor 10^4–10^6, will not be discussed either. The only exception will be events with $q_t \sim q_0$ of the order of a few GeV, which provide an appreciable contribution to the total cross sections. Here the quantity q_0 is not constant, but increases with increasing energy and can reach 7–8 GeV in the case of the superconducting supercollider working at $s^{1/2} = 40$ TeV.

Let us now return to the total cross sections. For three decades, the interaction between high-energy hadrons has been the province of reggeon phenomenology.[1] This approach is based on the theory of complex angular momenta and incorporates in the most consistent manner the restrictions imposed by unitarity and crossing symmetry. It leads to a unified description of total, elastic, and inelastic cross sections (i.e., multiple production cross sections).

Before the early 1970s, reggeon phenomenology was dominated by the idea of weak coupling.[2] This is the simplest case of the theory of complex angular momenta j, whereby the scattering amplitude A for asymptotically high energies $s \to \infty$ is determined by a simple pole in the j-plane, i.e., the Pomeranchuk pole known as the pomeron. In the j-representation, the pomeron exchange amplitude is $A_{\mathbb{P}}(j,t) = r(t)/(j - \alpha(t))$, whereas in the usual s, t-representation, we have

$$A_{\mathbb{P}}(j,\ t) = r\ (t)\ [(-s)^{\alpha(t)}\ + s^{\alpha(t)}]^{-1}\ (\sin \pi\alpha\ (t))^{-1}.$$

Moreover, for zero-angle scattering for which the square of the four-momentum transferred to the pomeron is $q^2 = t = 0$, the trajectory of the pomeron, i.e., the position of the pole $\alpha(t)$, passes through the unit point $\sigma_t = \mathrm{Im}(s,0)/s \propto s^{\alpha(0)-1}$ and the pomeron exchange cross section $\sigma_t = \mathrm{Im}\,A(s,0)/s \propto s^{\alpha(0)-1}$ is independent of energy. Since, apart from the momentum q, no quantum numbers are transmitted by the Pomeranchuk pole, it is also referred to as a vacuum pole. Corrections to the pole amplitude in the case of weak coupling are logarithmically small; $\sigma(s) = \sigma(\infty)(1 - O(1/\ln s))$, and we may say formally that, at high energies, the vacuum pole is an experimentally observable object. However, to ensure that the corrections to single-pole exchange remain small, we must impose a number of conditions on the vertices describing the interactions of pomerons. The main condition is that the three-pomeron vertex $G_{3\mathbb{P}}$ must tend to zero if the momenta transmitted by the vacuum poles are $t \to 0$. In other words, weak coupling does actually remain weak if and only if $^3G_{3\mathbb{P}3}(0) = 0$. The quantity $G_{3\mathbb{P}}$ can be determined experimentally from the diffraction dissociation cross section of one of the colliding hadrons $p + p \to p + X$ in the so-called three-reggeon region $s \gg M_X^2 \gg m_N^2$. The fact that, experimentally,[4,5] $G_{3\mathbb{P}}$ is not annulled[1)] was the first cloud on the horizon of reggeon phenomenology in the weak-coupling limit, and was for a time simply ignored,[6] especially since the absolute magnitude of the vertex $G_{3\mathbb{P}}(0) = r$ was found to be numerically small. In all other respects, the overall picture remained very attractive. The simple pole asymptotics and the clear multiperipheral model for the description of the pomeron by a sum of ladder diagrams constructed from ordinary pions[7–10] (the ρ, ω, A_2,... mesons participate in exchange in more complicated cases)[11] ensured that the picture was so convenient and customary that it was often completely identified with reggeistics and the theory of complex angular momenta.

Despite the fact that the situation is now appreciably more complicated and a considerable rise in cross sections at collider energies can only be described in terms of strong coupling[12] (in which case the leading singularity in the j-plane that determines the behavior of the hadron scattering amplitudes at high energies is now not simply the pole but

 0038-5670/89/060479-21$01.80

the cut), the baggage accumulated in the theory of complex angular momenta is widely used as before, and continues to be the basis for the great majority of models. Although the basic results of reggeistics are usually, for the sake of simplicity, demonstrated by considering the example of the pomeron ladder model, they are much more general and are derived at an almost axiomatic level from the assumptions of analyticity, causality, and minimal reduction of amplitudes with increasing virtual mass of the interacting particles.[13-16]

In the first Section of this review, we shall briefly discuss the current experimental situation and shall show that the scattering amplitude varies significantly in the collider energy range. In the language of the plane of impact parameters, i.e., if we carry out the Fourier transformation with respect to the transferred momentum q

$$f(s, b) = \frac{1}{8\pi^2} \int (A(s, q^2)\, e^{iqb}\, \frac{d^2q}{s}$$

and look upon the amplitude $f(s,b)$ as the distribution of the density of matter in the fast hadron,[2)] it is clear from the data that $f(s,b)$ increases with increasing energy and the shape of the distribution gradually changes from the Gaussian $f \propto \exp(-b^2/2B)$ to the θ-function $f \to i\theta(R(s) - b)$, and the value of $f(s,0)$ tends to its unitary limit. This phenomenon is referred to as the BEL effect[18]: the proton becomes blacker, larger, i.e., its radius $R(s)$ increases, and it acquires a sharp edge. We shall try in this review to understand the physical nature of the BEL effect. The word "understand" means in this context that we shall try to establish how this asymptotic behavior of hadron-hadron cross sections arises from the Lagrangian of quantum chromodynamics (QCD), which is now the generally accepted microscopic theory of strong interactions. Despite the fact that the problem of nonemission of quarks has not been finally solved in QCD, and the "secret" of confinement still forces us to use quantum chromodynamics only in the very limited form of QCD perturbation theory (the numerous experimental confirmations are also largely confined to this perturbation theory), the problem is still sensible even if we are concerned with large cross sections and the so-called soft processes. The point is that the characteristic transverse momenta encountered in multiple production of secondary hadrons increase with increasing energy (they constitute the main component of the total, and account for practically the entire inelastic cross section σ_{in}. According to the UA1 data obtained on the $Sp\bar{p}S$ collider at $s^{1/2} = 900$ GeV, hadron jets,[3)] i.e., groups of particles concentrated within a small solid angle (with a total transverse momentum p_t in excess of 5 GeV) are encountered in more than a quarter of the events.[19-20] Such events are usually assigned to the category of "high p_t." Short distances, for which the QCD coupling constant is $\alpha_s \ll 1$, are significant for such events, and this means that we can use QCD perturbation theory to describe them. In Section 6, we shall discuss one of the extreme cases in which the principal source of multiple hadron production is the emission of minijets with transverse momenta $q_t \sim q_0$. The quantity $q_0 \propto \exp(1.26\sqrt{\ln s})$ then rapidly increases with increasing energy. It is found in this approach that semihard processes with $q_t \sim q_0$, in which short distances are significant, are the source of ordinary (and not rare) events that were previously considered soft. It follows that our microscopic theory, i.e., the QCD perturbation theory, enables us to understand the character of the inelastic cross section and, hence, using the optical theorem (and the well established formalism of the theory of complex angular momenta), the behavior of the total and the diffraction cross sections, as well.

1.1. *The increase in cross section and in interaction range.* First, let us examine, at a purely qualitative level, the main features of the mechanism of a collision between fast particles that lead to an increase in the total cross section with increasing initial energy.

In lowest-order of perturbation theory in the coupling constant g, i.e., in the Born approximation (Fig. 1a), the interaction amplitude is determined by the exchange of a particle of momentum $q = p_1 - p_1'$:

$$M \propto g^2 \frac{D}{q^2 - m^2}.$$

At high energies, the main contribution to the spin part of the propagator D is provided by longitudinal polarizations directed along the momenta p_1 and p_2 and, if the spin on the exchanged particle is σ, the amplitude becomes $M \propto g^2 (p_1 p_2)^\sigma$. In other words: the exchange of a spin-zero particle gives $M \propto g^2$ whereas the exchange of a spin-one particle gives $M \propto g^2 s$ (where $s = (p_1 + p_2)^2$), i.e., the cross section is $\sigma \propto M^2/s^2 \sim$ const, and so on. Fortunately, we do not have point particles with spin greater than one (if we ignore gravitation), since otherwise the theory would be unrenormalizible. At the same time, for the exchange of a bound state (Fig. 1b), the effective spin of the state, i.e., the Regge trajectory $\alpha(q^2)$, depends on the transferred momentum q. For all trajectories that cross the experimentally observed hadrons, the intercept is $\alpha(0) < 1$, and the corresponding cross sections $\sigma_t \propto s^{\alpha(0)-1}$ decrease with increasing s. The increase in cross sections occurs because, as energy increases, we have new inelastic channels such as the production of pairs of new heavy particles ($N\bar{N}$) or pairs of heavy c and b quarks (see Fig. 2a), the production of a large number of new hadrons ($M_{2\to n}$; Fig. 2b), the production of jets of hadrons with high transverse momenta, and so on. However, we must remember that the increase in the cross section is strongly limited by the unitarity condition, i.e., the interaction probability at a given point in the space of impact parameters b_t cannot exceed unity.[4)] The increase in the cross section for constant b_t must therefore cease sooner or later (the initial flux is completely absorbed, $\mathrm{Im} f(b_t, s) = 1$), and the subsequent increase in σ_t is entirely due to the increase in the interaction range, i.e., the region in which $f(b_t,)$ is appreciably different from zero.

1.2. *Mechanism responsible for the increase in the interaction range.* In actual fact, we know only one mechanism for the increase in the interaction range. In one form or another, it is used in very different models and relies on diffu-

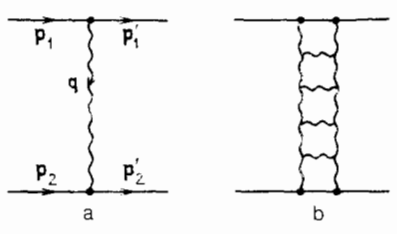

FIG. 1.

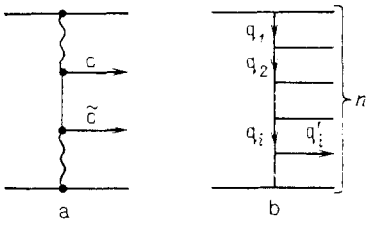

FIG. 2.

sion in the space of the impact parameters[8,21] b_t, which occurs in diagrams such as Fig. 2b when slower and slower intermediate particles (partons) are successively emitted. In each cell of the comb of Fig. 2b, i.e., in each emission, a parton is shifted in b_t space by the distance $\Delta b_t \sim 1/q_{ti}$, so that its mean distance from the center of the initial hadron after n steps is $(R^2)^{1/2} \approx [n(\Delta b_t)^2]^{1/2} \approx n^{1/2}/\langle q_t \rangle$ (in the ideal case, in which all the shifts take place in the same direction, we can have $R \sim n\Delta b_t \approx n/\langle q_t \rangle$). The characteristic number n of intermediate interactions increases logarithmically with increasing initial energy because the momenta $q_{i\parallel}$ decrease by a (finite) factor in each individual cell of the comb in Fig. 2b. In fact, we have $q_{i\parallel}/q_{i+1\parallel} = 1/x$ and $n = \ln(E_{in}/q_t)/\ln(1/x) = a \ln s$. The interaction range in the exchange of an individual reggeon is therefore given by

$$R^2 = n(\Delta b_t)^2 = \frac{a}{\langle q_t^2 \rangle} \ln s = R_0^2 + \alpha' \ln s.$$

1.3. *Parton cascades.* Diagrams such as those shown in Fig. 1b and 2b are usually regarded as an individual ladder (comb) in which there is only one slow parton for each rapidity level y. This is not correct. Each ladder contains a contribution in the form of a highly branched parton cascade (Fig. 3) containing a large number of slow partons. It is precisely the increase in the number of slow partons $N \propto s^{g^2K}$ that leads to the increase in the cross section $\sigma_t = N\sigma_0 \propto \sigma_0 s^{g^2K}$. On the other hand, Figs. 1b and 2b show, for the sake of simplicity, only one branch of the cascade of Fig. 3 (indicated by the thick line). It is actually the branch that leads to the formation of the parton that directly collides with the target. Let us illustrate these words with formulas (details can be found in Ref. 22). The cross section for the production of n particles in Fig. 2b is proportional to the square of the matrix element

$$|M|^2 = s^{2\sigma-2} \prod_{i=2}^{n+1} (g^2 K(q_i, q_{i-1})),$$

multiplied by the phase volume of secondary particles

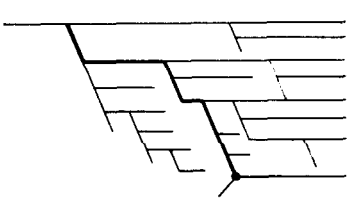

FIG. 3.

$$\sigma_n = s^{2\sigma-2} \int \prod_i g^2 K(q_i, q_{i-1}) \frac{d^3 q_i'}{E_i'}.$$

When the interaction constant g^2 is small, the ratio of transverse momenta $q_i/q_{i-1} \ll 1$ to the emission kernel K depends only on the transverse components q_{it}. If we fix the characteristic transverse momenta q_{it}, the cross section

$$\sigma_n = s^{2\sigma-2} \int \prod_i g^2 K \frac{dq_{i\parallel}'}{E_i'} = s^{2\sigma-2} (g^2 K \ln s)^n \frac{1}{n!}$$

is found to contain a logarithmic integral with respect to the secondary particles, $dq_{i\parallel}'/E_i' \approx \ln s$, and the total cross section is

$$\sigma_t = \sum_n \sigma_n \sim s^{2\sigma-2} \sum_n (g^2 K \ln s)^n \frac{1}{n!} = s^{g^2K+2\sigma-2}. \quad (1)$$

If particles of spin $\sigma = 1$, e.g., gluons, participate in the exchange, then even for $g^2 \ll 1$, the total cross section $\sigma_t = \sigma_0 (s/\langle q_t^2 \rangle)^{g^2K}$ will increase with increasing energy. The rise in the cross section is directly related to the increase in the number of slow partons. As the initial energy s increases, any parton can emit a new particle with probability $d\omega \propto g^2 K \, d\ln s$, and the overall multiplicity N is given by $dN = Ng^2K \, d\ln s$, i.e.,

$$N = N_0 \exp(g^2 K \ln s) = N_0 s^{g^2K}.$$

As a result of diffusion in b_t space, the distribution of slow partons in the plane of impact parameters is described by the expression

$$\frac{dN(b_t, \ln s)}{d^2 b_t} = \frac{N}{\pi B} \exp\left(-\frac{b_t^2}{B}\right) = N_0 \left(\frac{s}{\langle q_t^2 \rangle}\right)^{g^2K} \frac{\exp\{-b_t^2 [g^2 K \ln(s/\langle q_t^2 \rangle)]/\langle q_t^2 \rangle\}}{\pi g^2 K (\ln s/\langle q_t^2 \rangle)\langle q_t^2 \rangle}. \quad (2)$$

where $B = \bar{n}/\langle q_t^2 \rangle$, and the mean number of intermediate interactions is $\bar{n} = g^2 K \ln(s/\langle q_t^2 \rangle)$, which follows from the above formulas [see (1)].

We emphasize the difference between the symbols N and n. The interaction probability $\sigma = \sigma_0 N \propto s^{g^2K}$ is proportional to the total number N of slow partons in the branching cascade of Fig. 3. However, after collision, the side branches of the cascade (fine lines in Fig. 3), whose coherence has not been broken, assemble together again (into diagrams such as the self-energy or mass renormalization of ladder partons and the initial hadron), and the only particles that are emitted from the chain are those that have directly collided with the target (thick line in Fig. 3). The number n of these particles is equal to the number of intermediate interactions in an individual ladder and determines the multiplicity of secondary hadrons. The mean value $\bar{n}$ is conveniently calculated by taking the derivative of the logarithm of the cross section with respect to the logarithm of the constant g^2:

$$\bar{n} = \frac{d\ln\sigma}{d\ln g^2} = \sigma_0 \sum_n C_n n (g^2 K \ln s)^n \left[\sigma_0 \sum_n C_n (g^2 K \ln s)^n\right]^{-1}.$$

In our case, the coefficients are $C_n = 1/n!$ and the multiplicity is $n = g^2 K \ln s$.

1.4. *Screening.* If we look upon a nucleus consisting of

many nucleons as a set of a large number of slow partons, formulas (1) and (2) can be interpreted as the impulse approximation for the interaction of fast particles. They are valid only when the bare scattering cross section $\sigma_0 \propto g^2$ is so small that the scattrering amplitude, written in the impact parameter representation, is

$$f(b_t, s) \sim \sigma_0 N(b_t, s) \sim \sigma_0 s^{\omega_0 K} e^{-b_t^2/B} \ll 1 \qquad (3)$$

at any point b_t.

Since, with increasing energy, the cross section in the impulse approximation (1) increases without limit, the partons begin to screen one another with the result that the amplitude becomes $|f(b,s)| \leqslant 1$. From the standpoint of (3), this means that (3) remains valid only for large distances:

$$b_t^2 \geqslant Bg^2 K \ln s \sim (g^2 K \ln s)^2 \langle q_t^2 \rangle^{-1} = R^2 = (a \ln s)^2, \qquad (4)$$

whereas inside the circle $b_t < R$, the interaction probability $\operatorname{Im} f(b,s) \to 1$ is limited by the unitarity condition (the inident beam is completely absorbed).

The combined effect of diffusion in b_t space and of screening (s-channel unitarity) ensures that the effective interaction range [for increasing cross section (1)] becomes proportional to the logarithm of the energy $R \sim \langle q_t \rangle^{-1} g^2 K \ln s$, which was the case when the parton was always displaced in the same direction in each diffusion step. This is in fact the case. As we reach the edge of the disk $b_t \approx R$, we select from the large number of possibilities $N \propto s^{g^2 K}$ the cascade branch for which the particles are displaced in the same direction. For example, as the successive gluons are emitted (i.e., a parton decays into two), we select from the two new slower partons the one that moves to the right (the parton moving to the left is absorbed by the black disk in which $\operatorname{Im} f \to 1$). We emphasize that the logarithmic increase in the interaction range $R \propto \ln s$ is due to the outer branches of the parton cascade, i.e., particles that are always (for any rapidity y) at the edge of the disk filled with partons (in its own rapidity range). The particle density in this outer region is low ($|f(b,s)| < 1$), and screening effects have little qualitative influence on the picture described above. Screening and rescattering of partons can produce only a small reduction in the numerical coefficient $a \sim g^2/\langle q_t \rangle$, i.e., in the rate of increase in the range[5] $R = a \ln s$).

At asymptotically high energies, the amplitude $f(b,s)$ takes the form of a θ-function with a smooth edge [we shall denote it by $\tilde{\theta}$]: $\operatorname{Im} f(b,s) \approx 1$ for $b < R(s)$ and $|f| \ll 1$ for $b > R(s)$. Experiment confirms these tendencies and the behavior of the amplitude for the elastic scattering of high-energy protons. This is referred to as the BEL effect[18]: the proton becomes blacker ($\operatorname{Im} f(0,s) \to 1$), its edge becomes sharper ($f(b,s) \to i\theta(R - b)$), and its radius becomes larger ($dR/\mathrm{d} \ln s = a > 0$).

The above picture of the increase in cross sections is very general. Twenty five years ago one could doubt the validity of perturbation theory with large coupling constants $\lambda/m \sim 1$, when the ladder of scalar particles of Fig. 1b was considered as an example of a reggeon ($\lambda\varphi^3$ theory) and the large coupling constants were necessary to ensure that the cross sections did not decrease with increasing energy. Today, we have spin-one gluons in quantum chromodynamics, and we can readily obtain a growing cross section even for small constants $\alpha_s \ll 1$ for which the leading logarithmic approximation of QCD perturbation theory works satisfactorily.

Total cross sections of the form $\sigma_t \to 2\pi a^2 \ln^2 s$ are often said to show Froissart behavior or maximally rapid increase in cross sections (Froissart[23] has shown that the cross section cannot increase more rapidly than the square of the logarithm of energy). This is a limiting case of the strong coupling regime[12] $\sigma_t \propto (\ln s)^\beta$, $R \propto (\ln s)^\eta$, $\beta \leqslant 2\eta \leqslant 2$ for which $2\eta = \beta = 2$. Theoretically, we cannot exclude the situation ($\beta < 2\eta < 2$) in which, owing to numerous screenings and rescatterings of partons, the transparency of a fast hadron at the disk center becomes greater (i.e., $f(b_t,s) \to 0$ for $s \to \infty$ and $b_t < R(s)$) and the cross section increases more slowly than $\ln^2 s$. The so-called critical pomeron model[24-27] is an example of this situation. However, there is not a single satisfactory microscopic construction that leads to $0 < \beta < 2$, and, since we are interested not so much in the method of description of the data on the total hadron cross sections as in the dynamics of the increase in the cross section and the interaction range, we shall not examine this type of strong-coupling regime with an asymptotically transparent fast hadron ($\beta < 2\eta < 2$) any further.

For completeness of presentation, we record that Froissart derived his limitation in a much simpler way.[23] Thus, suppose that the bare scattering amplitude does not increase more rapidly than the square of the energy ($f_0 \leqslant Cs$). On the other hand, at very large distances, b_t, the amplitude decreases as $\exp(-2m_\pi b_t)$. The rate of decrease ($2m_\pi$) is determined by the position of the nearest singularity in the square of the transferred momenta $t = t_0 = 4m_\pi^2$. For distances

$$b_t > R = \frac{1}{2m_\pi} \ln s$$

the amplitude $f(b_t,s)$ is then sufficiently small (less than unity). For smaller b_t, the function $f(b_t,s)$ is bounded and the result is that the total cross section becomes

$$\sigma_t = 2 \int \operatorname{Im} f(b_t, s)\, d^2 b_t \leqslant 2\pi R^2 \sim \ln^2 s.$$

This type of increase in the interaction range, whereby the large bare amplitude $f_0 \propto s$ falls to values $f \sim 1$ allowed by unitarity only for

$$R \sim \frac{1}{2m_\pi} \ln s,$$

is very convenient if we are concerned only with fitting the experimental points. It is quite unsuitable for constructing a microscopic dynamic model. There are no point particles in QCD with spin greater than unity, and if such particles were to be introduced into the theory, it would become unrenormalizable and we would not know (at present) how to use it.

1.5. *Increase in transverse momentum.* We now return to quantum chromodynamics and consider the transverse momentum distribution of gluons in Figs. 1b and 2b. Since the coupling constant α_s is dimensionless in QCD, all the integrals (except one) with respect to the momenta of the newly created particles are logarithmic in character $(\int dq_{ti})^2/(q_{ti}^2 + q_{t,i+1}^2)$. The dimensions of the cross section $\sigma \propto 1/q_t^2$ are such that the denominator contains one superfluous q_t^2 and only integrals with respect to transverse momenta converge. In the intermediate branches of the comb,

significant values of q_{ti} are determined by transverse momenta of neighboring cells $q_{t,i} \sim q_{t,i\pm1}$. Because of asymmetry under the interchange of the ends of the diagram (up $\leftrightarrow$ down interchanges), the probabilities of emission of successive gluons with $q_{t,i+1}/q_{t,i} = z > 1$ and $q_{t,i}/q_{t,i+1} = z > 1$ are equal. In other words, the logarithm of the transverse momentum ($\ln q_{ti}$) can be altered at each stage with equal probability by an amount of the order of unity in either direction ($\Delta \ln q_{ti} \sim \pm 1$). With increasing number of comb cells, i.e., total multiplicity, a new phenomenon appears in QCD, namely, diffusion in the space of $\ln q_t$, first described in Ref. 28. This diffusion produces an increase in the mean value $\langle \ln q_t \rangle \propto n^{1/2}$ with increasing number of comb branches ($\ln^2 q_t \propto n$), and since the total multiplicity of the slow gluons in the cascade increases with energy ($N \propto s^{\bar{\omega}K}$), we find (as in the case of diffusion in the space of impact parameters) that, with probability of the order of one, the cascade contains[6)] a gluon with transverse momentum q_{ti} reaching q_0, whose logarithm is proportional to the number n of diffusion steps; $\ln q_0 \propto n \propto \alpha_s K \ln s$.

We shall later encounter the mean square gluon momentum $\langle q_{ti}^2 \rangle$. For a diffusion distribution of the form $(\pi n)^{1/2} e^{-2(\ln q_t/n)} d \ln q_t$, this mean is given by

$$\langle q_t^2 \rangle = \int \Lambda^2 e^{2\ln(q_t/\Lambda)} e^{-\ln^2 q_t/n} \frac{d \ln q_t}{\sqrt{\pi n}} = \Lambda^2 e^{n}.$$

The momentum q_0 introduced above can therefore be interpreted as the root mean square $\langle q_t^2 \rangle^{1/2} (\ln (q_0^2/\Lambda^2) = \ln \langle q_t^2/\Lambda^2 \rangle = n \propto \alpha_s K \ln s)$. If, in addition, we recall that the coupling constant (which determines the number of diffusion steps $n \propto \alpha_s y$ within the rapidity interval) depends on the transverse momentum as follows:

$$\alpha_s (q^2) = \frac{4\pi}{b \ln (q^2/\Lambda^2)},$$

we obtain the following law of increase in the characteristic momentum q_0 with increasing rapidity $y = \ln s$:

$$\ln \langle q_t^2 \rangle \backsim \alpha_s (q_t^2)\, y \backsim \frac{y}{\ln \langle y_t^2 \rangle},$$

i.e.,

$$\ln \langle q_t^2 \rangle \backsim y^{1/2}.$$

1.6. *Two types of diffusion.* It follows that, as the quark-gluon cascade of Fig. 3 develops, two types of diffusion occur in QCD, namely, diffusion in the space of impact parameters b_t and diffusion in the space of $\ln q_t$. It would not be correct to conclude that these two types of diffusion occur simultaneously. If we choose a cascade branch along which $\ln q_t$ increases, then the displacements $\Delta b_{ti} \sim 1/q_{ti}$ of partons in the transverse plane of this branch rapidly become negligible, and a chosen chain of partons "freezes" at the particular point in b_t space. This phenomenon is shown somewhat schematically in Fig. 4 where, along the vertical axis, we plot the rapidity y or, in the language of complex angular momenta, the imaginary diffusion time $it = y = \ln 1/x$ (x is the fraction of hadron momentum transported by the parton $x_i = q_i/q_n$) and the impact parameter b_t is plotted along the horizontal axis.

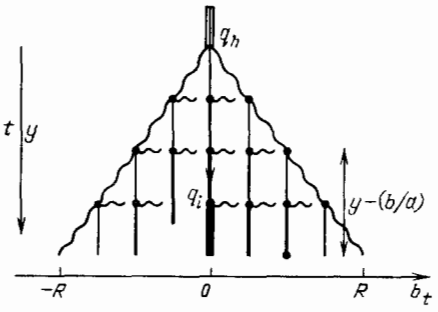

FIG. 4. Example of a quark-gluon cascade in the plane of rapidities y and impact parameters b_t. The line thickness is a measure of the increase in transverse momentum q_t.

The interaction range is increased by partons with relatively small transverse momenta[7)] $q_t \approx Q_0$ at the edge of the disk (sloping lines in Fig. 4), and vertical chains represent the cascade banches in which the transverse momentum q_t increases (the line thickness represents the increase in q_t). The probability of the reverse process, i.e., a reduction in q_d by diffusion in $\ln q_t$, followed the displacement of the given chain in the b_t plane toward the edge of the disk, is exceedingly small for the following reason. The density of partons (gluons and quarks) at the center of the disk is already close to saturation [$f(b_t, y) \to i$]. The partons sensibly screen one another in this region. The parton rescattering cross section $\sigma \propto 1/q_t^2$ increases as q_t decreases, and a parton with relatively low $q_t \ll q_0(b_t, y)$ in the central part of the disk collides with nearly 100% probability with neighboring gluons (quarks) having $q_t \sim q_0$. The parton thus again acquires $q_t \sim q_0$. Unfortunately, here we encounter a very complicated many-body problem with interaction and, so far, a parametrically exact answer (in α_s) for the parton distribution function in the central region has not been found. All that can be done at this point is to provide reasonable and reasonably argued hypotheses. Only the edges, i.e., the outer surface of the comb in Fig. 4 ($b_t > R(y)$), or the distribution of partons with relatively high transverse momenta $q_t > q_0(b_t, y)$, can be examined with sufficient rigor. In both cases, we select chains of partons along which b_t and the momentum q_t increase monotonically, and the density of partons and the probability of their redistribution are low along the entire chain[8)], so that screening effects can be taken into account by perturbation theory.

To conclude this Section, we describe once again how the parton wave function of a fast hadron is formed (see Fig. 4). Quarks and gluons emit successively slower and slower partons, i.e., mostly gluons with high color charge and spin 1. Initially, when $x \sim 1$, the partons have relatively low $q_t \sim Q_0$ and they first experience diffusion in the space of the impact parameters (first part of the interval of rapidity y), shifting by the distance $\Delta b_t \sim 1/Q_0$ in each step. Next, as a result of diffusion in the space of $\ln q_t$, the transverse momentum q_t begins to increase, the shift becomes $\Delta b_t \sim 1/q_t \to 0$, and for the remaining interval of rapidity $\bar{y} = y - (b_t/a)$ (disk radius $R = ay$), the impact parameter b_t remains practically constant, but the transverse momentum $q_t \approx q_0(b_t, y)$ continues to increase in accordance with the expression $\ln q_t \propto \bar{y}^{1/2} = [y - (b_t/a)]^{1/2}$.

The increase in the characteristic transverse momen-

tum $q_t \sim q_0(y)$ enables us to verify the validity of perturbation theory because the QCD coupling constant $\alpha_s(q_t) = 4\pi/b \ln q_t^2/\Lambda^2$ decreases with increasing q_t. We emphasize that the qualitative conclusion about the logarithmic rise in the interaction range $R \propto \ln s$ remains valid whatever the mechanism responsible for quark confinement.[9] Confinement can limit the range of momenta in which the QCD perturbation theory is valid, i.e., the minimum values of momenta $q_t \geqslant Q_0$ transmitted by the quarks (gluons), but slow partons can travel away from the center of a fast hadron to a distance $b_t \approx ay$ for any finite Q_0, so that the interaction range increases at the rate $dR/d \ln s \geqslant a \sim \alpha_s(Q_0)/Q_0$). The true rate of increase can be even greater because of processes with very small transferred momenta q_t. In particular, for $q_t \ll 1$ GeV, for which the language of quarks and gluons is no longer valid, an additional increase in the interaction range may be due to emission of pions (and other rare mesons) from the periphery of the disk. Their contribution will be disucssed in greater detail in Section 7.

1.7. *Theoretical problems.* (a) The first of these problems has already been discussed. In the central part of the disk, in which the rescattering of a large number of partons with $q_t < q_0(b_t, y)$ must be taken into account, the many-body problem with interaction cannot be solved exactly, and the exact parton distribution functions cannot be found. For the moment, estimates have to be based on models that are very reasonable, but are still only models. Fortunately, this is unimportant for many applications. All we need to know is that the region contains a large number of particles and that the total probability of interaction is close to unity, i.e., the disk becomes asymptotically black and $\mathrm{Im} f(b,s) \to 1$.

(b) The question that requires more detailed examination is the self-consistency of this picture from the standpoint of s-channel and t-channel unitarity, especially when diffraction dissociation is taken into account. Since a maximally rapid increase in cross section and interaction range constitute an extreme boundary condition for the strong coupling case, there are some doubts as to whether it is generally possible to construct an internally noncontradictory Froissart model (i.e., a model with cross section $\sigma_t \propto \ln^2 s$). These doubts appear to be well founded.

(1) We begin with the t-channel unitarity condition and examine the diagram of Fig. 5a which describes the jump in the elastic scattering amplitude at the nearest singularity, i.e., the cut near the point $t = 4m_\pi^2$. The contribution of the graph of Fig. 5a to the cross section is proportional to the product of the cross sections for the interaction between pions and the initial hadrons $\sigma(s_1)/\sigma(s_2)$ (shaded blocks in Fig. 5a). Because of the kinematic condition $s_1 s_2 \sim sq^2$, the pairing energies are $s_i \propto s^{1/2}$ and, if the cross sections $\sigma(s_i) \propto \ln^2 s_i$ grow rapidly, the coefficient in front of the singularity at the point $t = 4m_\pi^2$ decreases with energy more rapidly than the total cross section. In the representation of complex angular momenta j, the unitarity condition has the form

$$\frac{1}{2i}(f(j, t+i\varepsilon) - f(j, t-i\varepsilon)) = A(t-4m_\pi^2)^{j+(1/2)} \times j(j, t+i\varepsilon) f(j, t-i\varepsilon), \tag{5}$$

where $A = \text{const}$. The amplitude for froissarton exchange, i.e., a black disk of radius $R = a \ln s$, is

$$f(j, t) = \frac{a^2}{2[(j-1)^2 - a^2 t]^{3/2}}, \tag{6}$$

and, near the singularity at $j - 1 \to 2am_\pi$, the right-hand side of (5) is much greater than the left-hand side. For constant total cross sections and pomeron-dominated weak-coupling regime, the amplitude $f_{\mathbb{P}}(j,t) \propto 1/(j - \alpha(t))$ has the form of a pole and, since the singularity at $t = 4m_\pi^2$ appears on the trajectory $\alpha(t)$ itself, the jump in the amplitude $\Delta f_{\mathbb{P}} \propto \Delta\alpha(t)/(j - \alpha(t))^2$ has the same energy (j) dependence as the right-hand side of the unitarity condition (5). In the case of the froissarton, this simple solution of the consistency problem, which involves the introduction of the coefficient a into the singularity, cannot be carried out. However, it was noted in Refs. 29 and 30 that one can readily ensure that the right-hand side of (5) does not increase more rapidly than the left-hand side by taking into account in the expression for the range $R \approx ay$ an additional term proportional to $\ln y$:

$$R = ay - \beta \ln y. \tag{7}$$

For high energies $y \to \infty$, the second term $\beta \ln y$ is a small correction to the interaction range $R \approx ay \gg \beta \ln y$. However, the behavior of the amplitude $f(j,t)$ near the singularity $t \to 4m_\pi^2$ is now very different:

$$f(j, t) \propto (j - 1 - at^{1/2})^{t^{1/2}\beta - (3/2)} \approx (j - 1 - at^{1/2})^{1/2} \quad (\beta = m_\pi^{-1}),$$

and, for $j - 1 \to at^{1/2}$, the amplitude $f(j,t)$ becomes very small.

(2) Essentially the same problem arises in the case of the s-channel unitarity condition. Let us fix the point b_t on the edge of the disk in the space of impact parameters, at which the amplitude $|f(b_t, s)| \ll 1$ is numerically small and screening effects can be neglected, and let us evaluate at this point the contribution of diffraction dissociation (Fig. 5b). In the simplest form of the froissarton, the black disk has the radius $R = ay$, the amplitude $f(b,s)$ takes the form of a

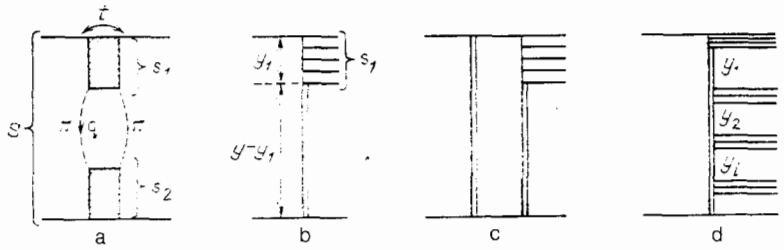

FIG. 5.

smoothed θ-function $f(b,s) = i\tilde{\theta}(R(s) - b)$ ($\tilde{\theta}(x) = 1$ for $x > 0$ and $\tilde{\theta}(x) \propto \exp(-2m_\pi x)$ for $x < 0$, and the total probability of diffraction dissociation is

$$G_0^D(b_1, s_1, s) \propto \int \operatorname{Im} f(b_1, y_1)|f(\mathbf{b} - \mathbf{b}_1, y - y_1)|^2 \, d^2b_1 \, dy_1$$
$$\propto yy^{1/2} \propto (\ln s)^{3/2} \quad (8)$$

and increases rapidly with increasing energy. At high energies, it becomes greater than the total probability $\operatorname{Im} f(b_1,s) \ll 1$. When the probability G^D given by (8) is calculated, the significant point is that the range is a linear function of the logarithm of energy, and the amplitude sum $R(y_1) + R(y - y_1) = ay = R(y)$ is equal to the total range $R(y)$. The factor $y^{1/2}$ appears after integration in the space of impact parameters d^2b_{1t}, and the factor y is due to integration with respect to the mass of the newly formed system of particles produced in the dissociation process $ds_1/s_1 = dy_1$.

Of course, we cannot assume that the probability of any particular subprocess exceeds the total probability of collision, since this would be in conflict with s-channel unitarity. in the interior of the black disk, in which the amplitude is $f(b_1,s) \to i$, the problem can be solved relatively simply. The contribution of the graph of Fig. 5b is completely screened by the diagram of Fig. 5c (Refs. 31 and 32), and the dissociation probability is

$$G_{0+b}^D = G_0^D |1 - \operatorname{Im} f(b_1, s)|^2 \to 0.$$

From the point of view of the multiple production cross sections, this means that we cannot observe pure dissociation in low partial waves with $l = (1/2)b_1 s^{1/2} \langle (1/2)Rs^{1/2} \rangle$. The collision of a few further partons always occurs at the same time, and the system breaks up completely, filling the accessible phase volume with secondary hadrons.[33]

In the outer region $b_1 > R(y)$, we again have the additional term $\beta \ln y$ in the range (7). The sum

$$R(y_1) + R(y - y_1) = ay - \beta \ln y_1 - \beta \ln (y - y_1)$$

is therefore now less than the total range[10]

$$R(y) = ay - \beta \ln y \; *), \quad (x)$$

and the amplitudes $f(b - b_1, y - y_1)$ and $f(b_1,y) \approx i\tilde{\theta}(R(y_1) -)b_1)$ fall exponentially in the region $b_1 > R(y)$, while the dissociation probability G^D is found to be less than the total probability $\operatorname{Im} f(b_1, s)$ (Ref. 30). Similar considerations apply to more complicated cases such as multi-reggeon processes[34,35] (Fig. 5d) in which several particle beams separated by large intervals of rapidity y_i are produced. These processes have been the cornerstone of verifications of the self-consistency of different Regge schemes. In particular, the necessity for restricting the increase in the cross section for multi-reggeon processes led to the requirement of annullment of multi-pomeron vertices (including G_{3P}) when the transverse momenta transmitted by the pomerons tend to zero.[3,36] Such contradictions can be avoided in modern models with maximally rapid increase in cross section and range given by (7), so that a self-consistent picture can be obtained that satisfies both the s-channel and t-channel unitarity conditions (at least on the nearest singularity $t = 4m_\pi^2$).

Moreover, by systematically taking into account diffraction dissociation, it is possible (using the method proposed in Ref. 30) to obtain an equation for the rate of increase in the interaction range $R(y)$ as a function of energy. The stable solution of this equation is then of the form given by (7), with the perfectly definite value $\beta = 1/m_\pi$.

2. DESCRIPTION OF EXPERIMENTAL DATA

In this and in the following Sections, we shall enumerate the basic experimental data on the increase in the cross sections and in the interaction range of high-energy hadrons, and will briefly discuss a number of typical models of the interaction between fast hadrons. Of course, the single fact that the cross section increases rapidly in the accessible energy range cannot be regarded as proof of the Froissart behavior of the hadron interaction cross sections at asymptotically high energies. However, the great majority of models describing modern data are found to reach the regime of maximally rapid increase in cross section $\sigma_t \ln^2 s$ as $s \to \infty$. On the other hand, since this behavior is naturally predicted by QCD, we shall adopt the Froissart asymptotic behavior as the basic working hypothesis.

2.1. *Total cross sections.* The first indications of an increase in the total cross sections with increasing energy were obtained on the Serpukhov accelerator when the cross section for the K^+p interaction was mesured.[36] The phenomenon has been referred to as the Serpukhov effect. It is no accident that the K^+p reaction has appeared at this point. According to the theory of complex angular momenta, the asymptotic behavior of the cross section is determined by the extreme right-hand side vacuum singularity of the scattering amplitude on the j-plane, and this behavior should be universal for all particles. However, the pre-asymptotic terms corresponding to the exchange of the so-called secondary ρ, ω, A_q, and f reggeon trajectories (which fall as $1/s^{1/2}$) depend on the quantum numbers of the colliding hadrons, and the contribution of secondary trajectories is found to be highly suppressed for K^+p. This is why the increase in the cross section with increasing energy was first noted in the K^+p interaction. It is important to note that the increase in σ_t with increasing energy had been predicted by the reggeon theory in which two possible asymptotic regimes were considered.[2,12] The first was the weak coupling regime in which a simple Pomeranchuk pole predominates for $s^{1/2} \to \infty$, and the cross section tends to a constant limit from below, i.e., $\sigma_t \to \text{const} - (a/\ln s)$. The second is the strong coupling regime in which the asymptotic cross section increases logarithmically, i.e., $\sigma_t \propto (\ln s)^\beta$ $(0 < \beta \leqslant 2)$.

For many years, the most popular alternative was the simpler weak coupling case, and the first Serpukhov data were successfully described within the framework of this approach.[37] However, new data on the increase in the πp and pp cross sections[38–40] appeared after the advent of the 400-GeV accelerators (FNAL and SpS) and the collider rings at CERN (ISR), and the impression was gained that the strong coupling regime was more probable in nature. This received general acceptance after measurements of σ_t were made at higher energies in the $Sp\bar{p}S$ proton-antiproton collider ($s^{1/2} = 0.2 - 0.9$ TeV; Refs. 41 and 42) and in cosmic rays[43,44] ($s^{1/2} \geqslant 30$ TeV). Figures 6a–c[11] provide some idea about the present state of σ_t data.

We shall now reproduce a number of expressions that

have been used to parametrize data on σ_t. One of the simplest and oldest of these is

$$\sigma_{NN} = 38{,}8 + 0.4\left(\ln\frac{s}{137\ \text{GeV}^2}\right)^2\ \text{mb}. \qquad (8')$$

More modern analyses have shown that

$$\sigma_{pp} = 36{,}1 + 19{,}5\left(\frac{s}{1\ \text{GeV}^2}\right)^{-1/2} + 0.39\ln^2\left(\frac{s}{44\ \text{GeV}^2}\right)\ (\text{mb}), \qquad (9)$$

$$\sigma_{pp} = 21{,}4 + 46{,}8\left(\frac{s}{s_0}\right)^{-0{,}25} - 16{,}3\left(\frac{s}{s_0}\right)^{-0{,}43} + 0{,}24\ln^{\beta}\frac{s}{s_0}\ (\text{mb}),$$

$$s_0 = 1\ \text{GeV}^2,\quad \beta = 1{,}096 \pm 0{,}014. \qquad (10)$$

The expression given by (8′) does not take into account the contribution of secondary trajectories. Instead, the very large value $s_0 = 137\ \text{GeV}^2$ was chosen, so that the reduction in the cross section for $s < 100$ GeV was specified by the term $\ln^2(s/s_0)$ although, of course, this reduction (due to the square of the logarithm) has no physical meaning; it is merely a simple approximation.

Secondary reggeons were taken into account[47] in (9). Finally, the exponent β in (10) was taken to be the adjustable parameter. As can be seen from the experiment, β approaches its maximum value $\beta = 2$ alloed by the Froissart limit. However, the coefficient in front of $\ln^2 s$ remains much smaller than the value π/m_{lab}^2 mb allowed by the Froissart limit.

2.2. *Slope of the diffraction cone.* Total cross sections are usually discussed together with a much wider set of data that are closely related to σ_t. This includes data on the real part of the scattering amplitude (the ratio $\rho = \text{Re}\,A/\text{Im}\,A$) and on the slope of the elastic cross section cone $d\sigma/dt (B = d\ln(d\sigma/dt)/dt)$. The slope is a measure of the interaction range $R^2 \propto B$. It is clear from Fig. 7, which plots measurements performed in the 1970s and the early 1980s, using the IFVE, FNAL, SpS, and ISR accelerators, that the interaction range increases with energy. The linear parametrization

$$B = B_0 + 2\alpha'\ln s, \qquad (11)$$

is usually employed for B. It is suggested by the weak coupling formulas for which one expects the asymptotic predominance of a single pole (the pomeron) at high energies. When the simplified expression (11) is employed, the quantity α' is often found to be different for different reactions (pp, $\bar{p}p$, πp), etc.) and different energy intervals. However, it was shown in Refs. 53 and 54 that, when secondary reggeon trajectories were taken into account in the range $s = 100$–$4000\ \text{GeV}^{-2}$, the same value $\alpha' = 0.12 \pm 0.03\ \text{GeV}^{-2}$ was obtained for the scattering of any pair of hadrons. This confirms the universal character of the leading vacuum singularity.

However, it is clear even from naive geometrical considerations, that the square of the interaction range cannot increase more slowly than the total cross section ($2\pi R^2 \geqslant \sigma_t$). This is the reason why, as the energy increases further, the formula for the slope B should acquire a term proportional to $\ln^2 s$ (or at least $(\ln s)^{\beta}$)[12] The following is an example of this type of parametrization:

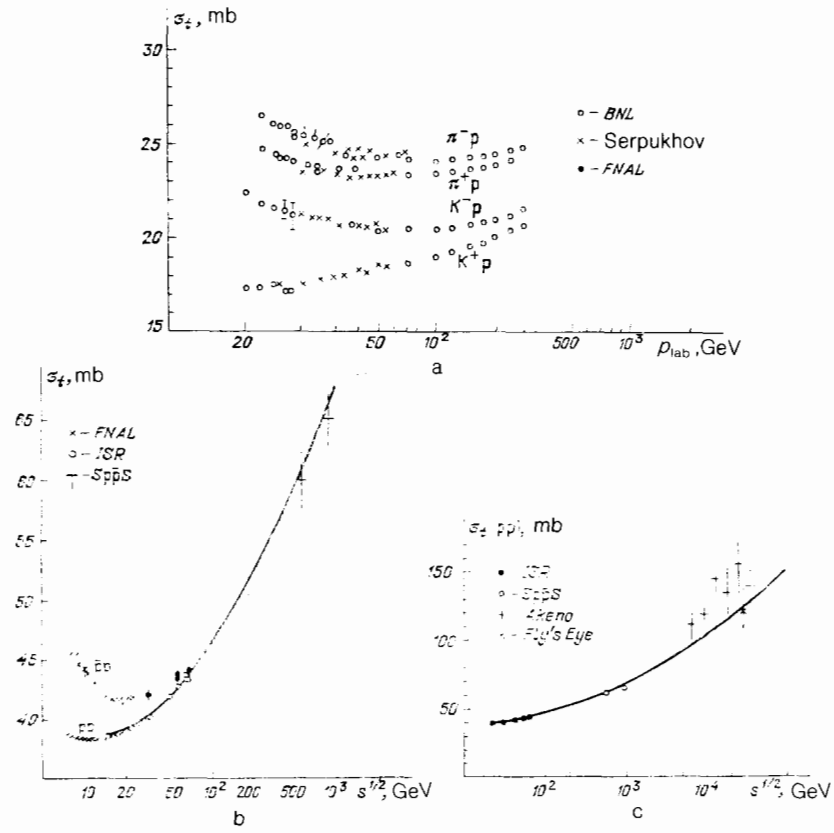

FIG. 6. Total cross section for *pp* scattering as a function of energy. Data taken from Refs. 38–44. Curve represents (10).

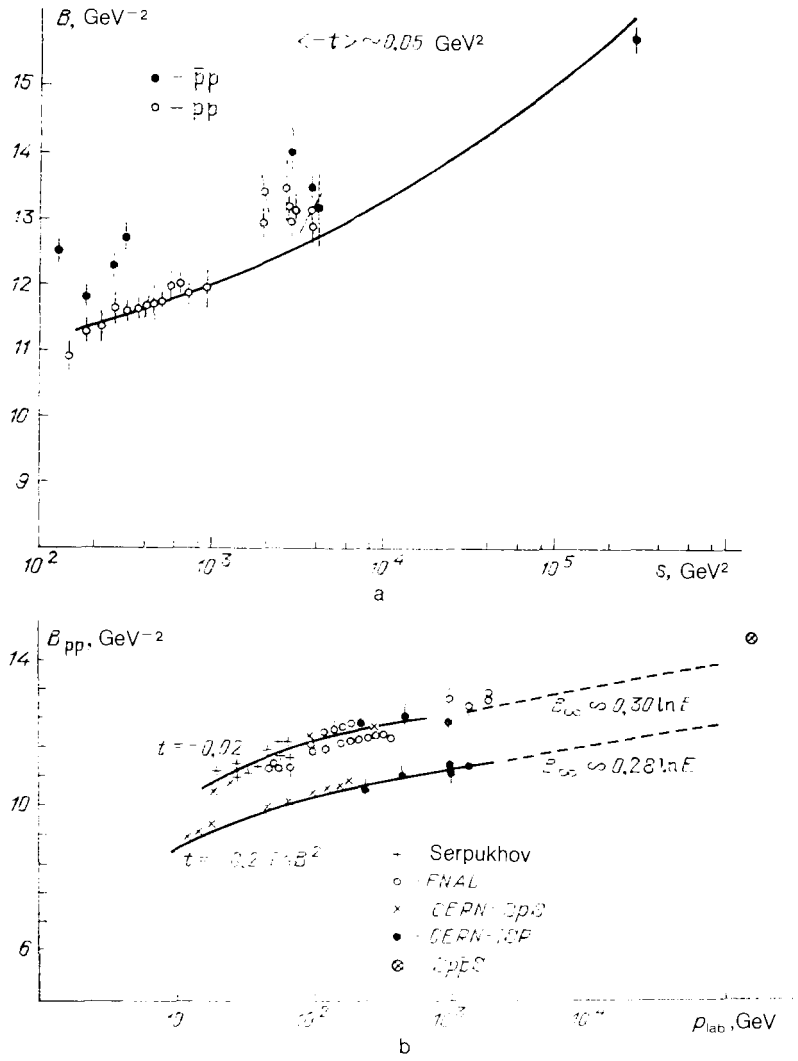

FIG. 7. Slope of diffraction cone for elastic pp (a,b) and $\bar{p}p$ (a) scattering as a function of energy. Data taken from Refs. 49–51. The curve of Fig. 7b represents (12).

$$B = 10.64 + 0.044 \ln^2 \frac{s}{s_0} \text{ GeV}^{-2} \quad (s_0 = 5 \text{ GeV}^2). \tag{12}$$

We note that, if the interaction between two hadrons at asymptotically high energies can be regarded as scattering by a black disk of radius R (and it is precisely this picture that we have been suggesting), the coefficients in front of $\ln^2 s$ in the formulas for the cross section (σ_2) and slope (b_2) are related by $\sigma_2 = 8\pi b_2$. From this point of view, the coefficients σ_2 and b_2 in (8) and (12) are in good agreement with one another. We now reproduce a further experimental "fact" or, more likely, an indication that, at high energies, the slope B increases in proportion to $\ln^2 s$. This was provided by EAS experiments[44,45] which have shown that $\sigma_{\text{in.}}(p - \text{Air}) = 540 \pm 40$ mb at $s^{1/2} \approx 10$ TeV. This cross section is significantly greater than the geometrical size of the nitrogen nucleus, i.e., $\pi R^2(^{14}\text{N}) \approx 200$ mb. This large cross section can only be explained by assuming that the range of the nucleon-nucleon interaction has increased to $B \approx 30$ GeV^{-2} (Refs. 55 and 56). If we interpret the slope in terms of the simple formula given by (11) within the interval $s^{1/2} = 1 - 30$ TeV, we find that $\alpha'_{\text{eff}} = 0.9$ GeV^{-2}. This sharp increase in α'_{eff} (for $s^{1/2} \approx 10 - 50$ GeV we use $\alpha'_{\text{eff}} \approx 0. - 0.2$ GeV^{-2}) is due to the fact that, in reality, the interaction range is proportional to the square of the logarithm of energy,[13] and $R^2 \propto \ln^2 s$).

2.3. *Real part of the scattering amplitude.* Let us now briefly consider the ratio Re A /Im A which is of particular interest because it allows more convincing extrapolation of existing experimental data to still higher energies. The point is that, owing to the analyticity of the scattering amplitude, the dispersion relations enable us to relate the real part of the amplitude and the discontinuity

$$\text{Re } A(s) = \frac{1}{2\pi} \int_{-\infty}^{+\infty} \frac{\text{disc } A(s')}{s' - s} \, ds'. \tag{13}$$

By using the unitarity condition and/or the optical theorem, we can express the discontinuity

$$\text{disc } A(t = 0) = 2 \text{ Im } A(t = 0) = 2\sigma_t s$$

in terms of the total interaction cross section. Moreover, the left and right cuts cancel one another almost completely at high energies if the only surviving amplitude is that with positive signature and equal values on left $s < -(m_1 + m_2)^2$ and right $s > (m_1 + m_2)^2$ cuts (i.e., $A(s) = A(-s)$). The only exception is the region of the

pole (s' close to s) whose contribution to the real part can be expressed in terms of the derivative of the total cross section

$$\operatorname{Re} A(s) \approx \frac{\pi}{2} s \frac{\partial \sigma(s)}{\partial \ln s}. \tag{14}$$

Thus, by measuring the ratio $\operatorname{Re} A / \operatorname{Im} A$, we actually obtain information on the rate of subsequent increase in the total cross section with energy. The data on $\operatorname{Re} A / \operatorname{Im} A$ are practically always taken into account when cross section data are fitted to a particular expression [see, for example, (8)–(10)]. Thus, measurements of the real part of the πp scattering amplitude[54] have been used to determine reliably the increase in the cross section at relatively low energies ($s = 100 - 600\ \text{GeV}^2$) and to extrapolate σ_t to higher values of s.

New data have now appeared on the real part of the $\bar{p}p$ scattering amplitude. For $s^{1/2} = 546$ GeV, the above ratio is found to be[57] $\operatorname{Re} A / \operatorname{Im} A = 0.24 \pm 0.04$, which is probably evidence for a more rapid [than indicated by the parametrization (8)–(10)] increase in the cross section for energies in the range $s^{1/2} = 0.5$–3 GeV. This increase in cross section was predicted by the model in Ref. 56 for $\Delta = \alpha(0) - 1 \approx 0.3$. A detailed discussion of the current situation with regard to $\operatorname{Re} A / \operatorname{Im} A$ can be found in Ref. 58.

2.4. *Amplitude in the impact parameter representation.* To gain a clearer idea about the change in the behavior of the interaction amplitude $A(s,t)$ of fast hadrons at higher energies, it is convenient to carry out the Fourier transformation and pass to the impact parameter representation:

$$f(b_t, s) = \frac{1}{8\pi^2 s} \int A(s, t)\, e^{i q_t b_t}\, d^2 q_t = \frac{1}{4\pi s} \int A(s, t)\, J_0(q_t b_t)\, q_t\, dq_t. \tag{15}$$

At high energies, the square of the transferred momentum $t = -q_t^2 + O(1/s)$ is equal to the square of the transverse momentum q_t. This tranformation contitutes the partial wave analysis of the elastic scattering amplitude. For each value of b_t, there is an orbital angular momentum

$$l = \frac{1}{2} b_t s^{1/2}.$$

The total and elastic cross sections can then be expressed in terms of the amplitude $f(b_t,s)$ as follows:

$$\sigma_t(s) = 4\pi \int b_t \operatorname{Im} f(b_t, s) db_t, \tag{16}$$

$$\sigma_{el} = 2\pi \int |f(b_t, s)|^2 b_t db_t \tag{17}$$

$$\sigma_{in} = 2\pi \int G_{in}(b_t, s) b_t db_t, \tag{18}$$

and the unitarity condition assumes the form

$$2 \operatorname{Im} f(b, s) = |f(b, s)|^2 + G_{in}(b, s), \tag{19}$$

where $G_{in}(b,s)$ represents the contribution of inelastic channels corresponding to the total angular momentum $l = (1/2) b s^{1/2}$. The function $f(b,s)$ is frequently written in terms of the complex scattering phase $f = i(1 - \exp(i\chi(b,s)))$ or, if we neglect the real part, in terms of the transparency $\Omega = \operatorname{Im}\chi$:

$$f(b, s) = i(1 - e^{-\Omega(b, s)}). \tag{20}$$

If, in addition, we neglect the dependence of the scattering amplitude on the spins of the colliding particles,[14] and suppose that the ratio $\operatorname{Re} A / \operatorname{Im} A = \rho$ remains constant (independent of q_t) in the significant part of the integration range in (15), we can readily find the amplitude $A(s,t)$ directly from the elastic differential cross section:

$$A = 4is(1 - i\rho) \left[\frac{d\sigma_{el}}{dt} (1 + \rho^2)^{-1} \right]^{1/2} \sqrt{\pi}, \tag{21}$$

and if we substitute this in (15) we obtain $f(b,s)$.

The corresponding analysis of the πp, Kp, πp, and $\bar{p}p$ scattering amplitudes was reported in Ref. 59. Here we confine our attention to $\bar{p}p$ and pp collisions for which there are data at the highest available energies, and show in Fig. 8 the function $G_{in}(b_t,s)$ that represents the probability of inelastic interaction for given impact parameter b_t. The most interesting aspect of this is the clear demonstration of breakdown in geometric scaling between the ISR energies ($s^{1/2} \sim 50$ GeV) and collider energies ($s^{1/2} \sim 500$ GeV). Geometric scaling was actively discussed in the middle 1970s (Refs. 60 and 61). The significance of the hypothesis is that, as the energy increases, the profile of the function $f(b_t,s)$ does not change, and only the interaction range becomes different, i.e., there is a change in the scale on which we measure the coordinate b_t, $f(b_t,s) = f(b_t/R(s))$. The hypothesis of geometric scaling is approximately satisfied for $s^{1/2} = 15 - 63$ GeV. One of its manifestations is the constancy of the ratio $\sigma_{el}/\sigma_t \approx 0.175$ (for pp scattering). However, this ratio rises to 0.215 ± 0.005 when the collider energy $s^{1/2} = 546$ GeV is reached.[41] The variation in the optical density of the proton is best seen in Fig. 8b which shows the increase in the function G_{in} (i.e., inelastic cross section) for a fixed ratio $b_t R(s)$ ($\Delta G = G_{in}(s_1) - G_{in}(s_2)$) in the ISR energy range $s^{1/2} = 23$ and 63 GeV, and the Sp$\bar{p}$S energy range $s_2^{1/2} = 546$–53 GeV. We note that the inelastic cross section increases for all values of (b_t). However, this increase is suppressed at the center of the disk $b_t \to 0$ at which the quantity G_{in} approaches its unitary limit ($G_{in} \leqslant 1$). The function G_{in} increases at its maximum rate at the edge of the disk ($b_t \sim 0.9$ fm). As already noted, this phenomenon was referred to as the BEL effect. In other words, the experiment showed a qualitative change in the profile of the fast hadron, which changes from a relatively transparent object with a Gaussian density ($G_{in} \propto \exp(-b_t^2/R^2(s))$ to a black disk with a relatively sharp edge. This means that, when we try to explain the increase in the cross sections, we must be able to understand two phenomena, namely, the increase in the interaction range $R(s)$ (large) and the increase in the cross section (black) within the disc $b_t < R(s)$.

3. MODELS FOR CROSS SECTIONS

There is a very wide spectrum of models aiming to describe different properties of hadron collision processes at high energies. A detailed discussion of each of them is beyond our scope here, and we shall confine our attention to a few, hopefully typical, examples. As a rule, there has been a tendency to concentrate attention on total (σ_t) and elastic cross sections $d\sigma/dt$ in the region of moderate $|t|$, and, less frequently, on polarization effects. Models constructed in the reggeon language[62,63] can be used together with the AGK reggeon cutting rules[14] (that connect the contributions of a given reggeon diagram to the total cross section and to the cross sections for events with particular secondar-

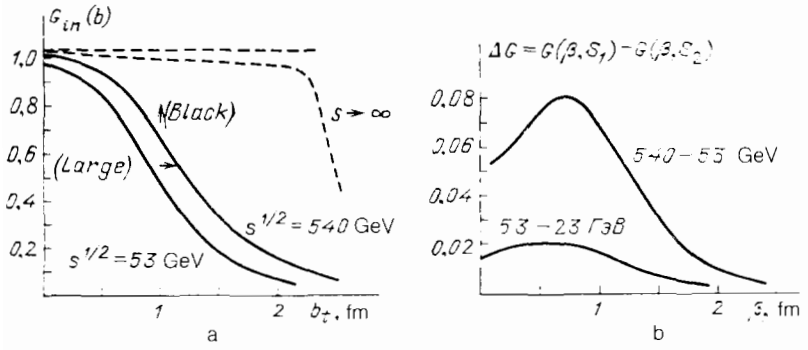

FIG. 8. *a*—Inelastic amplitude for the *pp* interaction G_{in} as a function of the impact parameter b_t; *b*—increase in the function G_{in} for energies in the range $s^{1/2} = 53 \div 23$ and $s^{1/2} = 540 \div 53$ GeV for fixed ratio of the impact parameter b_t to the interaction range $R \propto (B(s))^{1/2}$; $\beta = B_t (B(s_{max})/B(s_i))^{1/2}$. The lower curve in Fig. 8a refers to $s_1^{1/2}$ and the upper to $s_2^{1/2}$.

allel the distributions over the multiplicity N of the newly produced hadrons (i.e., the topological cross sections σ_N) and the inclusive cross sections $d\sigma/dx$ that reflect the distributions of secondary hadrons over the fraction of longitudinal momentum (i.e., rapidity) carried off by them.[15] The most complete and comprehensive description of data on two-particle reactions, including polarization and charge-transfer processes, can be found in the review by Kane and Seidl[64] in which the reggeon approach is used to carry out a detailed analysis of the energy dependence of the amplitude for two-particle reactions. In addition to the pomeron contribution, a detailed discussion is given of the role of secondary reggeon and multireggion cuts. Kane and Seidl were able to describe all the data available in 1975 (their review was published in 1976) on differential cross sections and polarizations at energies above 10 GeV. They did it by using in the vacuum channel the amplitude corresponding in the impact parameter representation to a disk of constant of optical density and a rounded edge (with disk radius given by $R^2 = R_0^2 + \alpha' \ln s$). The Sp$\bar{p}$S collider data were not available at the time, and this parametrization of the increase in the radius was found to be reasonable in a finite energy interval. Moreover, Kane *et al.*[64,65] were the first to predict correctly (in advance rather than to describe existing data) the magnitude and the very nontrivial t-dependence of polarization at the high energies of $E = 100$–300 TeV/c, including the high ($\sim 30\%$) polarization in the range $-t = 1.5$–2 GeV^2.

Modern models do not, as a rule, attempt to describe such a wide range of phenomena (the review of Kane and Seidl[64] covered practically all possible two-particle reactions). Special attention is usually devoted to the total and elastic cross sections for $\bar{p}p$ and pp collisions up to very highest energies. The characteristic property of the great majority of models is (see, for example, Refs. 66–72) the maximally rapid increase in total cross sections at asymptotically high energies, $\sigma_t \propto \ln^2 s$. Models based on the theory of the critical pomeron[24–26] constitute the exception. Here, the total cross section in the asymptotic region increases relatively slowly, i.e., $\sigma_t \propto (\ln s)^{(0.3}$, and the present day increase in the cross section is explained by the influence of pre-asymptotic threshold effects.[26,27,55,73] The amplitude for the exchange of one bare pomeron has its usual (pole) form only at relatively high energies for which $\xi = \ln(s/s_0)$ becomes greater than 3–5. However, although the theory of the critical pomeron refers formally to the strong coupling regime, it is ideologically closer to the weak coupling case (if we consider the way its constructed, i.e., by continuation in dimension from the logarithmic theory), and requires some "fine tuning", i.e., a number of specific relationships between the parameters of the bare pomeron trajectory and the values of multipomeron vertices have to be satisfied. By now. this type of "fine tuning" is neither reasonable nor necessary, and it seems to us that it is unlikely to be right despite the fact that, as yet, there are no serious experimental arguments against it. Other authors have used parametrizations of the scattering amplitude in which, in addition to the secondary trajectories, and, occasionally,[66] to a pomeron, use was made of the Froissart term corresponding to a black disk of radius proportional to the logarithm of energy.

It is assumed in Ref. 67 that only the edge of the disk is black and that its center becomes transparent as the energy increases. One of the defects of this model is the slow increase in the inelastic cross section $\sigma_{in} \propto \ln s$ while the total cross section is $\sigma_t \approx \sigma_{el} \propto \ln^2 s$. In the model proposed in Ref. 68, a double Pomeranchuk pole (Kiev dipole) is proposed in place of the Froissart amplitude. This amplitude corresponds to the logarithmic increase in the cross section and in the square of the interaction range at high energies: $\sigma_t \propto R^2 \propto \ln s$.

However, to describe Sp$\bar{p}$S collider data, the trajectory of the dipole pomeron must still be shifted by one to the right (the intercept of the trajectory is $\alpha(0) = 1.046$),[69] after which the cross section and the square of the interaction range begin to increase ($\sigma_t \propto R^2 \propto \ln^2 s$).

Despite the great diversity of the different expressions that are being used (this is clear even from the very brief enumeration that we have given), all the models describe satisfactorily the total and elastic cross sections at the FANL-ISR and Sp$\bar{p}$S collider energies ($s^{1/2} \geqslant 20$ GeV and $s^{1/2} = 0.2$–0.9 TeV, respectively). The behavior of elastic cross sections is also occasionally satisfactorily described even beyond the second diffraction peak, i.e., up to $|t| = 5$ GeV^2 (Refs. 69–72). It is interesting that a further C-odd amplitude (i.e., amplitude with negative signature), known as the odderon, has had to be introduced in these models to reproduce the differences between elastic cross sections for $\bar{p}p$ and pp scattering in the region of the diffraction maximum $s^{1/2} = 53$ GeV^2 (we now have data at $t \approx -1.3$ GeV). Three-gluon exchange, with each pair in a symmetric figure of eight in color, plays the part of this amplitude in quantum chromodynamics. The contribution of the odderon is dominant for large $|t|$ in the region of the second maximum $|t| > 1.5$ GeV^2, but the cross section in this region is then very small, i.e., lower than $d\sigma_{el}/dt$ by 4–6 orders of magnitude at 0° (Refs. 74 and 75).

We note that the authors of Ref. 70 used a parametriza-

tion of the elastic amplitudes which, for large transferred momenta t ensured that the differential cross section was in agreement with the simplest graphs (lowest orders) of QCD perturbation theory.

The asymptotic form of the scattering amplitude has often been used[62,63,76–78] to describe the interaction between partons (quarks and gluons in the colliding particles) and not the initial hadrons. The models described in Refs. 76–78 are interesting in that they assume that the parton-parton interaction cross section is $\sigma(\mathrm{gg}) = \mathrm{const}$ and is described by a simple Pomeranchuk pole. The increase in the cross section $\sigma_t = N_{ga} N_{gb} \sigma(\mathrm{gg})$ is then achieved by introducing logarithmically increasing gluon multiplicity ($N_g \propto \ln s$) into the wave functions of hadrons a and b. However, if the gluon interaction cross section is described in terms of QCD perturbation theory, this procedure leads to a double counting of graphs because, in the leading logarithmic approximation, the increase in multiplicity N_g, for example, is due to the same ladder diagrams[28,79,80] that represent the gluon interaction amplitude.[28] The models used in Refs. 62 and 63 are free from this defect and involve only the scattering of valence quarks. Since the quark-quark interaction amplitude is then written in reggeon language in the form of the sum of multipomeron exchanges, we have the opportunity of following in detail the relation between the total cross section and the inelastic interaction channels, i.e., we can calculate the cross sections for processes with different secondary hadron multiplicity σ_N and, starting with the structure functions for the distribution of valence quarks in the initial protons, successively reproduce the inclusive spectra of newly created pions, kaons, and nucleons as functions of the fraction of longitudinal momentum $\mathrm{d}\sigma/\mathrm{d}s$ carried off by them.[62] The diffraction dissociation cross sections are also discussed in the most recent papers from the ITEF group.[81]

4. REASONS FOR THE INCREASE IN σ_t IN MODELS

In most of the models enumerated above, the increase in the total cross section is actually postulated in advance. The elastic scattering amplitude includes the Froissart cut [of the form given by (6)], which is done, for example, in Refs. 66 and 70–71, or the pomeron exchanges with intercept $\alpha(0) = 1 + \Delta > 1$ (Refs. 62, 63, and 69). After unitarization,[16)] such exchanges in turn lead to the Froissart behavior of the cross section

$$\sigma_t = \sigma_0 + c \ln^2 s.$$

If we now turn to the microscopic level of analysis, we find that the following explanations of the increase in the cross section are now the most popular: (1) relaxation of thresholds for the production of heavy particles and (2) production of jets of hadrons with high transverse momenta.

The production of kaon-antikaon and nucleon-antinucleon pairs,[82] charm[73] or b-mesons, and even glueballs with mass of the order of a few GeV (Ref. 83) have been discussed at different times as new thresholds for the production of heavy particles. Of course, each individual threshold can ensure an increase in the cross section only over a very restricted energy interval, so that a large number of different thresholds is necessary to cover currently existing data. This was done, for example, in models based on the theory of the critical pomeron,[24–27,73] in which the asymptotic increase in the total cross section $\sigma_t \propto (\ln s)^{0.3}$ was found to be insufficiently rapid for energies in the range $s^{1/2} = 50$–900 GeV.

The trouble with this approach is that, on the one hand, an infinite number of new thresholds is necessary if the increase in the cross sections continues into the asymptotic energy range (EAS data[44,45] suggest that the increase in cross section continues up to $s \sim 10^9$ GeV^2). On the other hand, the cross sections for the production of antinucleons,[84] charm,[85] etc., are small in comparison with the cross sections for processes with high p_t (the probability of emission of a gluon with high p_{tg} is greater by more than an order of magnitude than for a heavy quark for $m_q = p_{tg}$). In the $\mathrm{Sp\bar{p}S}$ collider energy range ($s^{1/2} = 0.2$–0.9 TeV), the cross section for the emission of jets with $p_{tj} > 5$ GeV was found to rise from 2.4 to 10 mb in the central range of rapidities $|\eta| < 1.5$ alone. The advantages of high p_t include the absence of a clearly defined jet production threshold. Jets with higher p_{tj} can be emitted as the energy increases.

The idea that the production of particles with high p_t is the main reason for the increase in cross section was discussed[86,87] as far back as 1973–1975. A model based on the QCD perturbation theory and the gluon exchange mechanism was proposed later and was successful in describing the increase in the cross section up to collider energy $s^{1/2} \approx 0.5$ TeV (Refs. 88 and 89). It is interesting that, although the characteristic transverse momentum of gluon jets emitted in an inelastic collision in this model increases with increasing energy, it reaches only $q_{t\,\mathrm{jet}} = 2$ GeV when $s^{1/2} = 0.9$ TeV. However, the total transverse energy of all the jets in an event, $E_t = \Sigma |q_{tj}|$, is approximately 15–18 GeV, which is in reasonable agreement with experiment.

However, as noted above, an increase in the optical density of the proton (blackening) and in the interaction range was observed at high energies, and by exploiting only the thresholds for the production of new and increasingly heavy particles or jets with high q_{tj}, we can select central collisions with small impact parameter b_t. In particular, the inelastic cross section was found in Ref. 88 to increase by 17 mb (between $s^{1/2} = 30$ and $s^{1/2} = 500$ GeV) due to the transverse momenta $q_t^2 > 1.5$ GeV^2 alone.[17)] These q_t values correspond geometrically to a disk of area $\pi r^2 \sim 4\pi/q_t^2 \approx 3$ mb, which is in clear conflict with the unitarity condition. Moreover, it was predicted that the cross section would reach 1000 mb for $s^{1/2} = 10^{15}$ GeV, although the authors of this model gave no reasons for the greater interaction range. The fact that $\sigma_{in} = 1000$ mb is still below the formal Froissart limit[23] $(\pi/m_\pi^2) \ln^2 s$ is not a justification because the unitarity condition (19) has been violated for fixed values $b_t < 1$. The increase in cross section due to the blackening of the disc for fixed b_t must eventually stop because of the restriction $G_{in} = 2\,\mathrm{Im} f(b) - |f(b)|^2 = 1$ (there is no such thing as blacker than black).

It is thus necessary to increase the interaction range, and this can only be achieved for moderate q_t because the rate of diffusion in the space of impact parameters b_t is determined by the elementary shift per step $\Delta b_t \sim 1/q_t$ (see Sec. 1.3). We now have another question, namely, can we confine our attention to soft processes with low q_t and obtain a cross section that increases with energy by summing the ladder diagrams such as those of Fig. 2b, (i.e., the amplitudes for the production of a large number of hadrons $M_{2\to n}$) directly

in the hadron language? This seems quite possible if the interaction constant is high enough.

A single chain of Fig. 1b could alone ensure an increase in the total cross section. However, the actual cross sections for strong interactions at low energies (of the order of the masses of resonances $s_{ii+1} \sim 1$–5 GeV^2) are relatively low. Calculations based on a simple model with π-exchange,[7] including ρ, f, and g resonances with the bare amplitude for the $\pi\pi$ interaction, led to a cross section that fell with energy as $\sigma_t \propto s^{-0}$ (Ref. 90). To obtain at least a constant cross section, the model must include bare pion scattering blocks of very high (but finite) energy, i.e., the production of heavy clusters, or fireballs,[9,91] elastic $\pi\pi$ scattering blocks due to pomeron exchange,[10] and inelastic pion interactions due to the more complicated multiperipheral chain[11] that includes exchange and emission of ρ, ω, f and A_2 mesons (or, more precisely, the exchange of the corresponding Regge trajectories). The common feature of all these models is that it is impossible to remain in the region of very small transferred momenta $q_t \sim m_\pi$. The characteristic q_t increase with increasing pairing energy and are determined by the masses of the radiated resonances,[11,92] as demonstrated for the simplest model in Refs. 7 and 90. Typical values of q^2 are close to the mass of the ρ meson and may exceed 1 GeV^2 if special formfactors that restrict the values of q_t are not introduced. Since elementary soft interactions (for the experimentally determined coupling constants) cannot ensure a cross section that increass with energy, and we still have to introduce into the model the bare blocks for particle-scattering at relatively high energies and relatively high transferred momenta, it is natural to proceed in a different way, that is suggested by experimental data. The blackening of the disk at each fixed point of b_t space is due to processes with large q_t [as noted above, the cross sections for the production of jets with $q_t \geqslant 5$ GeV reach 10 mb for $s^{1/2} = 900$ GeV (Refs. 19 and 20), but only in the central range of rapidities $|\eta| < 1.5$], and the increase in the interaction range is due to diffusion in the impact parameter space of gluons with transverse momenta $q_t \sim 1$ GeV. We emphasize that the increase in the interaction range is indeed due to diffusion in b_t space, i.e., a series of successive emission of soft gluons, as described in Section 1, and not in a single jump.

In recent publications,[93,94] the Froissart increase in the interaction range was achieved by an over-simplified measure. The amplitude for the hard scattering of partons was first calculated from QCD perturbation theory ($q_t > q_{\text{hard}}$; this amplitude corresponds to the cross section $\hat{\sigma}$ that increases as a power function of energy, but has a very small interaction range $b_t \sim 1/q_{\text{hard}}$). The result was then "smeared out" over the impact parameter plane in accordance with the electric charge density of the initial hadrons, and this produced the eikonal function

$$\Omega(b_t, s) = \operatorname{Im}\chi(b_t, s) = \frac{1}{2} A(b_t)\,\hat{\sigma}_{\text{hard}}(\hat{s}), \qquad (22)$$

where

$$A(b) = \int \rho_a(\mathbf{b} - \mathbf{b}')\rho_b(\mathbf{b}')\mathrm{d}^2\mathbf{b}'$$

is the convolution of the two distributions of matter density of the colliding particles a and b [specifically, $\rho(b)$ is replaced with the electric charge density found from formfactor data]. Formula (20) is then used to construct the elastic scattering amplitude $f(b_t, s)$. The amplitude eikonalized in the spirit of the paper by Cheng and Wu[95] does not violate the two-particle s-channel unitarity condition (19) and provides a reasonable description of the total cross section data obtained from ISR, Sp$\bar{\text{p}}$S, and cosmic-ray data ($s^{1/2} = 10^2$–10^5 GeV). However, we still have to ask: what is the origin of inconsistency of such models? The large interaction range is specified right at the beginning, when the factored expression (22) is postulated by selecting the parton on the distant periphery of the hadron, i.e., by selecting a parton that has jumped to a large distance on the first diffusion step. The low probabilty $\sim\exp(-2m_\pi b_t)$ of this jump is balanced in (22) and (20) by the large cross section of the parton-parton interaction $\hat{s}_{\text{hard}}(\hat{\sigma}) \propto \hat{s}^{K\alpha_s(q_{\text{hard}})}$. However, if we apply the Froissart restriction directly to the parton-parton cross section[18] $\hat{\sigma}$, we see that it cannot then increase more rapidly than $\ln^2\hat{s}$ ($\hat{\sigma} \leqslant 2\pi\hat{R}^2 \hat{R} < c \ln \hat{s}$). This is confirmed by a detailed analysis of the diagrams that take into account screening and rescattering of the partons themselves. We thus see that the maximum interaction range that is due to the convolution (22), i.e., the distance $\Delta\bar{b}_t$, on which the function $\Omega(b_t, s) \sim O(1)$ is still not small, does not increase with energy more rapidly than $\Delta\bar{b}_t \propto \ln\ln\hat{s}$, or, more precisely, $\Delta\bar{b} \sim \ln\hat{R}$, where $\hat{R}$ is the parton-parton collision radius $\hat{R} < q_{\text{hard}}^{-1} \ln\hat{s}$. As can be seen, $\hat{R} \gg \Delta\bar{b}$ at high energies, and the main effect of the increase in radius is due to diffusion in b_t space and not to a single jump of the initial parton (valence quark) in the wave function of the fast hadron. From the point of view of unitarity, the substitution of the rapidly increasing cross section $\hat{\sigma}_{\text{hard}} \propto \hat{s}^{K\alpha_s}$ in (22) is equivalent to trying to balance the probability $\hat{\omega}$ of a collision of a pair of partons (quarks), which exceeds unity, by the fact that such events are very rare at large distances b_t from the center of the hadron, and the average probability $\omega(b_t) = \hat{\omega}A(b_t)$ (evaluated over all events) is less than unity. However, this argument is essentially fallacious. Each elementary subprocess must have a probability $\hat{\omega} < 1$.

A detailed examination of the conditions for the validity of such models (eikonal summation of diagrams corresponding to the exchange of pomerons with intercept of the trajectory $\alpha(0) = 1 + \Delta > 1$) can be found in the book of Abramovskii *et al.*[96] They show, in particular, that this scheme will work only in a restricted interva of rapidity ($\ln s < 1/\Delta$). We note that this last restriction also applies to the models of Refs. 62 and 63.

Finally, our point is that, at high energies, the increase in the interaction range is due to diffusion (on the b_t plane) of gluons with transverse momenta ~ 1 GeV (and to a lesser extent, to the emission of pions from the periphery of the hadron), and the blackening of the disk at a fixed point b_t is due to the creation of hadron jets with relatively large $q_t \sim q_0(b_t, s)$, where q_0 is the momentum reached as a result of diffusion in the space of $\ln q_t$ ($q_0 \propto (\ln s)^{1/2}$; see Section 1.6). In support of our point of view that even questions such as the increase in the cross section and in the interaction range can be reasonably discussed in the gluon language within the framework of the QCD perturbation theory, we note that if we take the data on the rate of contraction of the diffraction cone,[54] the coefficient in front of $\ln^2 s$, which is proportional to the square of the reciprocal of the transverse proton momentum on the periphery of the hadron, 0.043

$\mathrm{GeV}^{-2} \propto (\alpha_s/q_t)^2$, is found to be very small and corresponds to momenta $q_t \approx 1-2$ GeV. Even at energies in the range $s^{1/2} = 10$–60 GeV, which are not ultrahigh, the universal slope of the vacuum trajectory α' ($B = B_0 + 2\alpha' \ln s$) exceeds by only a small amount the minimum value[97] (at the point $t = 4m_\pi^2$)

$$\alpha'_{\min} = \frac{3}{2}\frac{\sigma_{\pi\pi}}{32\pi^3}\ln\frac{4m_\pi^2}{m_\rho^2} \approx 0.08 \ \mathrm{GeV}^{-2} \tag{23}$$

allowed by the t-channel unitarity condition. Experiment[53] shows that $\alpha' = 0.13 \pm 0.02\ \mathrm{GeV}^{-2}$. It is also clear that α' is largely determined by the relatively rare pion production events on the periphery of the hadron, and that the characteristic transverse momenta of the partons, i.e., quarks and gluons ($\alpha' - \alpha'_{\min} \sim \alpha_s/q_t^2$) are so high ($\gtrsim 1$ GeV), that we are fully justified in using the QCD perturbation theory. It may be said that the QCD Lagrangian enables us to reconstruct the high-energy hadron-hadron collision with the same degree of understanding of the interaction dynamics that had previously been achieved in quantum electrodynamics.

Of course, we are concerned only with a qualitative understanding of the interaction picture. At present day energies, the precision of calculations performed in the higher orders of QCD perturbation theory, or even in the leading logarithmic QCD approximation, is relatively low. It is controlled by the quantity $N_c\sigma_s(q^2)$ and, as a rule, does not exceed 30–50% whereas, in electrodynamics, the characteristic parameter is $\alpha_{EM} = 1/137 < 1\%$. The inclusion of higher-order corrections in the constant α is extremely laborious and we cannot at present expect the QCD perturbation theory to produce precise predictions. Neverhteles, the QCD Lagrangian gives us a very good understanding of the collision dynamics of fast particles, especially since the characteristic values of q^2 increase asymptotically with increasing energy, and the constant $\alpha_q(a^2)$ decreases. The picture that emerges from all this is very unusual. Questions such as the asymptotic behavior of the total cross section, the interaction range, and the cross section for the multiple production of hadrons, which are traditional in the physics of soft processes, are now found to be associated with the region of internal transverse momenta[19] $q^2 \geqslant 2\ \mathrm{GeV}^2$ and are found to be within the jurisdiction of QCD perturbation theory [coupling constant $\alpha_s(q^2 > 2\mathrm{GeV}^2) < 1/4$].

5. INTERACTION OF FAST HADRONS IN QCD PERTURBATION THEORY

5.1. *The equation for the cross section.* Equation (24) describes the evolution of the parton wave function of the fast hadron with increasing logarithm of its energy or, in other words, with increasing fraction of the initial hadron momentum that is carried off by an individual soft parton. It provides a reasonable basis for a microscopic dynamic model of the interaction between fast hadrons. For the sake of simplicity, partons will be understood to be exclusively gluons whose contribution predominates although the production of quark-antiquark pairs and the scattering of quarks are also significant and must be taken into account in calculations[98,99]

$$\frac{\partial\varphi(x,q,b)}{\partial\ln(1/x)} = \int K(q,q')\varphi(x,q',b')\exp\left[\frac{(\mathbf{b}-\mathbf{b}')_t^2 q_t'^2}{4}\right] \times q'^2 d^2b' N_c\alpha_s(q')\left(1-\frac{\alpha_s\varphi(x,q,b)}{\varphi_0}\right)d^2q'\cdot\frac{1}{4\pi^3} \tag{24}$$

where $\varphi(x,q,b)$ represents the cross section for the interaction of a gluon (or, more precisely, the probability density for interaction at the point $q = b_t$ in the space of impact parameters), subject to the condition that the transverse momentum transferred to the gluon in the uppermost cell of the ladder of Fig. 9a is given by $q_t^2 = q^2$.

The effect of the kernel K is as follows:

$$K(q,q')\varphi(q'^2) = \frac{\varphi(q'^2)}{(\mathbf{q}-\mathbf{q}')_t^2} - \frac{q_t^2\varphi(q^2)}{(\mathbf{q}-\mathbf{q}')_t^2[q_t'^2+(\mathbf{q}-\mathbf{q}')_t^2]}. \tag{25}$$

This kernel was obtained in Ref. 28 in the leading logarithmic approximation ($\mathrm{LLA_E}$) of QCD (in the energy) and sums all the diagrams that contain on each step of the small coupling constant α_s, the logarithm of energy

$$\ln\frac{1}{x} = \ln\frac{2mE}{q^2},$$

i.e., contributions of the form

$$\sum_n C_n\left(\alpha_s\ln\frac{1}{x}\right)^n.$$

The first term on the right-hand side of (25) corresponds to the emission of a new gluon and the second to the reggeization of the t-channel gluon that performs the exchange, i.e., the emission of a virtual gluon such as that shown in Fig. 9b ($N_c = 3$ is the number of colors). The factor $1 - (\alpha_s\varphi/\varphi_0)$ represents the interaction between the partons, i.e., the rescattering of gluons and their mutual screening. In the course of iteration of (25), the term $\alpha_s\varphi/\varphi_0$ generates a set of fan-shaped semi-enhanced diagrams such as those shown in Fig. 9b. The numerical value of $\varphi_0 = \mathrm{const}$ is determined by the effective three-ladder vertex G_{329P} calculated in $\mathrm{LLA_E}$ in Refs. 99 and 100. The physical significance of the factor $1 - (\alpha_s\varphi/\varphi_0)$ is that, in the region in which the probability density for the parton interaction is already high ($\varphi \sim \varphi_0/\alpha_s$), the introduction of the new reaction channel, i.e., the emission of a new gluon does not give rise to greater overall collision probability, but simply redistributes the probability among different subprocesses.

Finally, consider the factor $\exp[-(\mathbf{b}-\mathbf{b}')_t^2 q_t'^2/4]$. It is introduced to describe the displacement of the gluon in the plane of the impact parameters, i.e., diffusion in b_t. Strictly speaking, in quantum mechanics, the uncertainty relation $\Delta q\Delta x \sim \hbar$ shows that both the momentum q_t and the coordi-

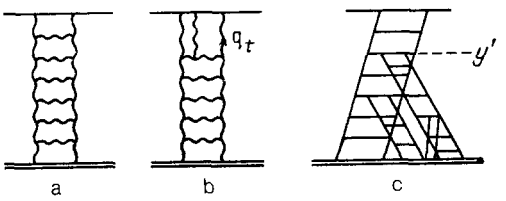

FIG. 9.

nate b_t cannot be simultaneously introduced. However, the large number of soft partons in the problem, $N \propto \exp[K\alpha_s \ln(1/x)]$, means that we can use both q_t and b_t with quasiclassical precision because, for the mean values evaluated over the ensemble, the uncertainty relation assumes the form[20] $\Delta\bar{q}\Delta\bar{x} \sim \hbar/N$. Since the coordinates b_t are quasiclassical, we chose the parton probability in the transverse plane in the form of the Gaussian $\exp(-\Delta b_t^2 q_t'^2/4)$.

If we neglect the factor $1 - (\alpha_s\varphi/\varphi_0)$, i.e., confine our attention to $\varphi \leqslant \varphi_0$, and integrate with respect to the impact parameter b_t ($\int \exp[-(b-b')^2 q'^2/4] d^2b' q'^2/4\pi = 1$), we find that $\bar{\varphi}(q) = \int \varphi(q,b) d^2b$ is given by the well-known Lipatov-Kuraev–Fadin LLA_E equation[28]

$$\frac{\partial \bar{\varphi}(x, q)}{\partial \ln(1/x)} = \int K(q, q') \bar{\varphi}(x, q') N_c \alpha_s(q') dq'^2/\pi. \quad (26)$$

Equation (24) describes two diffusions. First, it describes the diffusion in the transverse b_t plane and, second, in the plane of the logarithm of transverse momentum ($\ln q_t$). The integral with respect to q' converges for $q' \sim q$. For $\varphi_f \propto q^{2(f-1)}$, we have

$$\int K(q, q') \varphi_f(q') dq'^2 = \chi(f) \varphi_f(q),$$

with the eigenvalue given by

$$\chi(f) = 2\Psi(1) - \Psi(f) - \Psi(1-f) \quad (27)$$

$\Psi(f) = d \ln \Gamma(f)/df$, and $\Gamma(f)$ is the Euler gamma-function. When $\varphi \propto (q'^2)^{-1/2}$, which corresponds to the extremum of the function χ, significant values of $\ln q'$ differ from $\ln q$ by ± 1 and a kind of diffusion takes place in the space of $\ln q_t$ during iteration of equations (24) or (26) (see Ref. 28). As $s \to \infty$, the mean number of steps in this diffusion [linear equation (26)] becomes asymptotically $n = 4N_c\alpha_s(\ln 2/\pi) \ln s$, and the width of the distribution in $\ln q_t^2$ is $\Delta = 14\zeta(3)n/\ln 2$

$$\bar{\varphi} \sim \exp\left[\frac{4N_c\alpha_s \ln 2}{\pi} \ln s - \frac{\ln^2(q_t^2/Q_0^2)}{\Delta}\right]. \quad (28)$$

where the Riemann zeta-function is $\zeta(3) = 1.202$.

5.2. *Parton wave function of a fast hadron.* At low energies, the probability of an interaction with a parton carrying the fraction $x \sim 1$ of momentum (i.e., $\ln(1/x) \approx 0$) is small ($\varphi \sim \alpha_s < \varphi_0$) and is concentrated in a restricted region of b_t space. Typical transverse momenta are $\ln q_t \sim \ln Q_0$. As the energy ($\ln x^{-1}$) increases, equation (24) shows that ϕ increases monotonically because of the exponential increase in the number of slow gluons, $N \propto \exp[(\chi(N_c\alpha_s/(\pi)] \ln x^{-1}$, and the above two diffusions ensure that the gluons propagate within an increasing interval of transverse momenta [$\ln q_t^2/Q_0^2 \sim \Delta^{1/2}$; see (28)] and impact parameters $b_t^2 \sim n\langle 4/q'^2\rangle$. The diffusions in b_t and $\ln q_t$ occur sequentially rather than simultaneously. As $\ln(q_t'/Q_0)$ increases, there is a sharp drop in the rate of diffusion in the transverse plane $\Delta b_t \sim 1/q_t'$, so that on the first few steps (i.e., the cells of the ladder of Fig. 4), diffusion in the impact parameter b_t plays the main part so long as the transverse momenta $q_t' \sim Q_0$ are still relatively small. During this time ($\ln x^{-1}$), gluons are displaced to a distance R ranging up to

$$R \approx \frac{n}{Q_0} = \frac{\chi N_c \alpha_s}{\pi Q_0} \ln\frac{1}{x} = a \ln\frac{1}{x}, \quad (29)$$

after which diffusion in $\ln q_t$ comes into play. The mean transverse momentum increases, and the subsequent development of this branch of the gluon cascade occurs at a practically fixed point b_t. Interestingly, this picture is effectively very close to that of Amati *et al.*[101,102] who investigated the elastic scattering amplitude in the language of the reggeon field theory[13] in the situation in which the bare-pomeron intercept was $\alpha(0) = 1 + \Delta > 1$. The quasiclassical asymptotic behavior and summation over semi-enhanced diagrams[101] were also found to play an important role in their solution, and the final answer took the form of the θ-function $f(b,s) = i\theta(R(s) - b)$, where $R = a \ln s$. At each stage of the pomeron interaction, i.e., on the interval $dy \propto 1/\Delta = 1/\alpha(0) - 1$, the radius $R(s)$ of the disk increases as a result of the emission of new pomerons by the outer side of the disk. The parton density at the point b_t in then found to increase (the disk becomes blacker) because of the large pomeron intercept $\alpha(0) > 1$.

An even deeper analogy can be established with the theory of the heavy pomeron[103] in which each individual bare pomeron is rigidly fixed at a given point on the b_t plane, just as if it were constructed from particles with very high transverse momenta.

However, a useful property of chromodynamics, i.e., the asymptotic freedom of particles with high q_t, was not used in Refs. 101–103, so that the authors of these publications could only discuss a restricted range of questions by solving the self-consistency problem and postulating in advance the energy dependence of the amplitude for the exchange of the bare pomeron.

The increase in the function ϕ slows down for $\varphi \geqslant \varphi_0$, and finally ceases altogether when $\varphi = \varphi_{max} = \varphi_0/\alpha_s(q_t)$. For $\varphi > \varphi_{max}$, the factor $1 - (\alpha_s\varphi/\varphi_0)$ ensures that the derivative $\partial\varphi/\partial \ln x^{-1}$ changes sign and, according to (24), the function ϕ begins to decrease, again approaching ϕ_{max}. Detailed analysis[104] shows that, for given slow-gluon rapidity $y = \ln x^{-1}$, the function ϕ reaches ϕ_0 at points with coordinates $b_t \leqslant R(y, = ay)$ and

$$\frac{1}{\Lambda} \ln q_t = \frac{1}{\Lambda} \ln q_0(b_t, y) = 1.78\left(y - \frac{b_t}{a}\right)^{1/2}. \quad (30)$$

This means that, at distances ($b_t < a_y$) from the center of the incident hadron, the parton wave function of the fast hadron contains soft gluons with transverse momenta $q_0(b_t, y)$ with probability of the order of unity. At large distances b_t, or in the region of large $q_t > q_0(b_t, y)$, the probability of interaction with the corresponding parton is small.

Thus, from the parton point of view, a fast hadron is an almost black disk of radius $R = ay$. The balckness in the interior of the disk increases as a result of the increase in the density of gluons with large q_t ($\ln q_t/\Lambda \approx \ln q_0/\Lambda \sim 1.78y^{1/2}$), and the disk radius increases due to gluons with $q_t \sim Q_0 \sim$ const. We are thus able to reproduce the above phenomenon that is now referred to as the BEL effect.

We shall stipulate that equation (24) is valid (it can be justified in LLA-QCD) and is parametrically (in the constant $\alpha_s \ll 1$ exact only at the edges of the disk for $b_t > ay$ or for $q_t > q_0(b_t, y)$, where the gluon density is low ($\varphi \ll \varphi_{max}$). Here the situation is actually dominated exclusively by the ladder graphs and the semi-enhanced branching[99] of Fig. 9. For lower $q_t < q_0(b_t, y)$, the probability of different rescatterings of gluons is very high, and we must take into account all the possible enhanced multiladder diagrams. The problem cannot as yet be solved exactly.

In the central region $q_t < q_0(b_t, y)$, equation (24) can be regarded as a simplified model. The advantages of the model are: (1) it can be joined directly to the region of large $q_t \gg q_0$ (in which the validity of the QCD perturbation theory has been verified) or large impact parameters $b_t > ay$ (for which the proton density is low) and (2) the solution of (24) does not violate anywhere at least the two-particle unitarity condition (19).

We provide one more argument in support of the assertion that, for numerically large transverse momenta $q(m \ll q_t < q_0(b_t, y))$, the interaction probability $\varphi(x, q_t, b_t)$ is practically constant or, more precisely, $\varphi = \varphi_{\max}$.

The increase in the interaction probability ϕ is due to the fact that, as the energy increases, any parton can emit a further new and slower gluon, and the total multiplicity of soft gluons increases (if screening is ignored) in accordance with the law $dN = N\alpha_s N_c(\chi/\pi) d \ln x^{-1}$.

In the region in which we are interested here, the coupling constant is $\alpha_s \ll 1$, but it cannot be neglected because its smallness is balanced by the large kinematically accessible phase volume $d \ln(1/x)$. In the leading logarithmic approximation, the characteristic parameter is the product $\alpha_s \ln(1/x)$, which is not small. In the space-time picture, the large logarithm arises from integration with respect to the time τ of emission of the new gluon[105] which, because of the uncertainty relation, is given by $\tau_i \sim 2E_i/q_t^2$ and can vary from the finite value $\tau_u \sim 1/\mu$ to the lifetime of the parent parton $\tau_b \sim 2E/q^2$. Thus, with logarithmic precision, we have

$$\ln \frac{1}{x} = \int_{\tau_u}^{\tau_b} \frac{d\tau}{\tau} = \ln \frac{2mE}{q^2}. \tag{31}$$

However, to obtain this result, we must ensure that the gluon is radiated coherently throughout the entire time interval up to τ_b. If one or several collisions take place within this interval between the initial parent parton and other partons in the wave function of the original hadron (e.g., via the simple single-gluon exchange of Fig. 1a), the condition for coherent emission will be violated, the gluon will change its color, and the upper limit of the logarithmic integral (31) must be replaced with the typical mean free time τ_r. For relatively small $q_t < q_0(b, y)$, the parton density is high, and even for rapidity y' such that our transverse momentum is $q_t^2 = q_0^2(b_t, y'(/\alpha_s))$, the gluon experiences, on average, at least one collision during its lifetime $\tau_b(y') \approx \tau_u e^{y'}$. The time $\tau_b(y')$ characterizes the typical mean free path $\tau_r \approx \tau_b(y') = \tau_u e^{y'}$, which, in turn, is the upper limit of the logarithmic integral (31). Further increase in the rapidity interval does not lead to a logarithmically strong coherent emission of new gluons, and the parton density, i.e., the function $\varphi(x, q, b)$, remains practically constant and equal to the value of the function $\varphi(x', q_t, b_t) = \varphi_{\max}(q_t)$ at x' as the momentum fraction x decreases, where $q_0^2(x', b_t) = \alpha_s q_t^2$ (small nonlogarithmic corrections $\sim \alpha_s < 1$ are assumed to be negligible in LLA).

5.3. *Rate of increase in the interaction range.* We must now consider one further question. On the periphery of the disk $b_t = ay$, on which gluons with moderate $q_t \approx Q_0$ are concentrated, diffusion in the space of $\ln q_t$ cannot in general occur in both directions and lead to both an increase and a reduction in the transverse momentum of the gluon. Diffusion in the direction of very small q_t must be restricted. This limitation (gluon emission amplitudes with small q_t) is imposed, first, by the confinement mechanism, and second (and apparently much earlier) by the fact that small q_t are suppressed in the parton rescattering process. When it collides with one of the partons of virtuality and transverse momentum $q^2 \sim q_0^2(y, b)$, a gluon with lower momentum $q_t < q_0$ acquires additional transferred momentum $\Delta q_t \sim q_0$ and, since the probability of interaction with such partons $q \sim q_0$ is of the order of unity, most of the gluons are concentrated in the momentum range $q_t \sim q_0(y, b_t)$. Actually, there are few particles with high momenta $q_t \gg q_0(y, b_t)$ in the solution of (24), and particles with lower $q_t \ll q_0$ acquire $q_t \sim q_0$ after only the first rescattering.[21] From now on, it will be convenient to use the following parametrization of the momentum q_0:

$$q_0^2(x, b_t) = Q_0^2 + \Lambda^2 \exp(3{,}56\bar{y}^{1/2}), \tag{32}$$

where $\bar{y} = \ln(1/3x) - (b_t/a)$.

Strictly speaking, in LLA, we are essentially using only the leading exponential term $\ln q_0^2 = 3.56\ [\ln(1/x)]^{1/2}$, where the coefficient 3.56 is calculated from $N_c = 3$ and the number of species of light quarks with mass $m_q \ll q_0$ is $n_F = 3$. The pre-asymptotic terms Q_0^2 and the coefficient 1/3 are introduced arbitrarily into (32). The replacement of $\ln(1/x)$ with $\ln(1/3x)$ reflects the fact that the momentum of the soft gluon is naturally ascribed not to the momentum of the incident nucleon, p_N, but to the momentum of the valence quark $p(\langle p \rangle \approx p_N/3)$, and the term Q_0^2 represents the mean transverse momenta of gluons (in the hadron wave function) for which the interaction probability ϕ is no longer small (it approaches $\varphi = \varphi_0$). Since such values of ϕ (the blackening of the disk) are achieved for sufficiently soft gluons only after several diffusion steps in the space of $\ln q_t$ which increases[22] the significant values of q_t, the value of Q_0 will exceed by a substantial factor the bare transverse momentum q_{in} of valence quarks in the hadron, so that, by taking $q_{in} = 300$ MeV, we may expect that $Q_0 \approx 5q_{in} \approx 1.5$ GeV (Ref. 104). Of course, this is only a very coarse estimate. The first few graphs of the QCD perturbation theory do not suffice for accurate calculations, and the constant q_0 must be regarded within the framework of the LLA as an independent adjustable parameter. By processing the data on the production of hadrons with high transverse momenta $p_t \sim 2$–10 GeV at the $Sp\bar{p}S$ collider energy $Ns^{1/2} = 540$ GeV, we found that $Q_0 = 1.4$ GeV, which is very close to the original estimate. It is commonly considered that momenta $q_t \sim Q_0 \sim 1.5$ GeV are high enough to ensure that the entire discussion can be carried out in the language of quarks and gluons, and that the cross sections can be calculated with the QCD Lagrangian. Substituting the value $Q_0 = 1.4$ GeV that determines the minimum momentum $q_0(y, b_t)$ in (29), which describes in accordance with (24) the increase in the interaction range $R = ay$ with energy, we obtain

$$a = 0.40\ \text{GeV}^{-1}.$$

The measured increase in the interaction range corresponds to[18] $a = 0.42\ \text{GeV}^{-1}$. The agreement with experiment must be regarded as too good for our very simplified picture.

6. MULTIPLE PRODUCTION OF SECONDARY HADRONS

6.1. *Inclusive spectra.* To demonstrate the fact that the above picture correctly reproduces the interaction dynamics of fast hadrons and reflects the main features of the increase in total cross sections, let us consider the inclusive secondary-particle spectra. We note, first, that the main source of hadrons in this scheme is the fragmentation of gluon jets with $q_t \sim q_0$. For the $Sp\bar{p}S$ collider energies in the central region ($\eta = 0$), $s^{1/2} = 540$ GeV, we have $q_0 = 2.5$ GeV, whereas for the UNK ($s^{1/2} = 6$), the result is $q_0 = 4.5$ GeV. Finally, for the supercollider ($s^{1/2} = 40$ TeV), we find that $q_0 = 7$ GeV. It is precisely the production of gluon jets with $q_t \sim q_0$ that is the main reason for the increase in the total cross sections (the blackening of the central part of the disk and the increase in the interaction range due to gluons with $q_t \sim q_0(y, b_t \approx ay) \approx Q_0$ on the periphery of the disk). Jets with transverse momenta $q_t \gtrsim 5$ GeV are now referred to as minijets. The cross section for their production is very high. Experimentally, even at $s^{1/2} = 900$ GeV, about 40% of the events contain at least one jet with $q_{tj} \geqslant 5$ GeV in the pseudorapidity interval $|\eta| < 3 (\eta = -\ln \operatorname{tg}(\theta/2))$.

The inclusive cross section[19] $d^2\sigma^j/d\eta dq_t = 0.4 \pm 0.15$ mb/GeV for $\eta = 0$, $q_t = 5$ TeV, $s^{1/2} = 0.54$ TeV is in good agreement with the predicted result $d^2\sigma^j/d\eta dq_t = 0.55$ mb/GeV.

We emphasize that the cluster (group of particles with high resultant q_t) selected in the experiment and called a jet does not always coincide with the jet of hadrons produced during the fragmentation of an individual gluon or quark. There is a high probability that the group of particles we call a jet acquires one or a few extraneous pions from the fragmentation of neighboring gluons or, conversely, relatively slow particles (with $q_t \ll q_0$) are missed from their own jet. Moreover, fluctuations in the multiplicity and momentum distributions of hadrons in soft collisions can also simulate jet events. For example, it is reported in Ref. 106 that all minijets and, in particular, the UA2 data, can be described in terms of fluctuations. However, this approach employs phenomenological distributions (taken from the same experiment) on multiplicity that are already influenced by the fact of minijet production. In the wider kinematics of the UA1 experiment, the totality of the minijets cannot be explained in terms of fluctuations even by using the experimental two-particle correlations and multiplicity distributions of secondary hadrons in the simulation algorithm. The algorithm reproduces only about 70–80% of the jets with $q_{tj} = 5$ GeV and less than 35% of jets with $q_{tj} = 10$ GeV (Ref. 107). It is obvious that, by proceeding in this way, and by taking into account all the more complicated measured correlations, we will in the end reconstruct the hadron jet, and merely refer to it as a "fluctuation" in a soft process. To be fair, we must formulate the conclusion of Ref. 106 more accurately: "the experimentally observed minijets cannot be looked upon as experimental evidence for the existence of a new component in inelastic hadron-hadron collisions." We are in full agreement with this conclusion. From our point of view, the main source of secondary hadrons in ordinary "soft" events are indeed minijets with $q_t \sim q_0$. However, since experimentally it is practically impossible to select uniquely a minijet with low q_t (according to the UA1 estimates, about 18% of jets with $q_{tj} = 5$ GeV selected by their method were due to random fluctuations),[107] it is better to proceed to the description of the spectra of individual hadrons produced as a result of the decay of these minijets, and thus achieve a more precise determination of the parameters and a more direct comparison with experiment. Here we shall have to use the structure functions $\bar{D}_c(z)$ describing the fragmentation of a gluon jet into a hadron c that carries away a fraction $q_c/q_j = z$ of the momentum of the jet. The simple phenomenological function $\bar{D}_c(z) = (1-z)^2/z$ will suffice for a jet with moderate q_{tj}. In the case of large q_{tj}, we must also take into account the emission of additional gluons (and quarks) during the usual LLA evolution in $\ln q_{tj}^2$ (Refs. 79 and 80), and observe the conditions of angular ordering that arise (again within the framework of LLA) from the interference between coherently emitted gluons.[106–108] Using the formulas given in Ref. 99, and the expression for $q_0(x)$ averaged over the impact parameters b_t [cf. (32)],

$$q_0^2(x) = Q_0^2 + \Lambda^2 \exp\left[3{,}56\left(\ln\frac{1}{3x}\right)^{1/2}\right], \qquad (33)$$

we were able to describe the experimental data on the cross sections $d\sigma/dq_t^2$ and $d\sigma/d\eta$ in a wide energy range ($s^{1/2}$ between 50 and 900 GeV), on the assumption that all the secondary hadrons, even those with low $q_t \sim 300$ MeV, were produced exclusively as a result of the fragmentation of gluon jets.[109] The corresponding curves are shown in Fig. 10.

The curves of Fig. 10 were constructed by using only two adjustable parameters (which are not fixed within the framework of the LLA method). The value $Q_0^2 = 2$ GeV^2 determines the initial virtuality of the partons, the cross section scale $\sigma \propto 1/Q_0^2$, and also the rate of increase of the cross section with energy, both for the total cross section [the coefficient a in the formula $R = ay$ (29), $\sigma_t \to 2\pi R^2$] and the inclusive cross section $d\sigma/d\eta$ shown in Fig. 10b.

The second parameter Λ determines the scale along the q_t axis and the magnitude of the coupling constant $\alpha_s(q^2) = 4\pi/b \ln(q^2/\Lambda^2)$. The value that we have obtained, $\Lambda = 52$ MeV, is equivalent to taking $\alpha_s = 0.16 \pm 0.01$ at $q^2 = 22.5$ GeV^2 from Ref. 113.

It is interesting to note that the mean transverse momentum of secondary particles is also found to increase with increasing multiplicity N in a given event. Actually, the increase in N is achieved either as a result of a more frequent emission of gluons, i.e., an increase in the number n of diffusion steps in the interval of rapidity y, which immediately produces higher q_t because $\langle \ln^2 q_t \rangle \propto n$, or by producing several cascade branches at once (diagrams that respond to the branchings of Fig. 11 in the language of the reggeon diagram technique). However, the graphs of Fig. 11 involve additional logarithmic integrations with respect to the transverse momenta Q_t transferred along individual reggeons (ladders) and a diffusion in the space of $\ln Q_{it}$. Since the momentum Q_{it} plays the part of initial virtuality Q_0 for its own comb, the mean q_t of secondary particles increases[109] with increasing number m of combs (Fig. 12). The distributions over the number of charged particles are also satisfactorily described in this picture (Fig. 13), but this involves the further parameter $g = 0.37$ that represents the probability of production of an extra cascade branch $p_m \propto g^m$.

We note that all three adjustable parameters (Q_0, Λ, and g) assume very reasonable and natural values, and agree

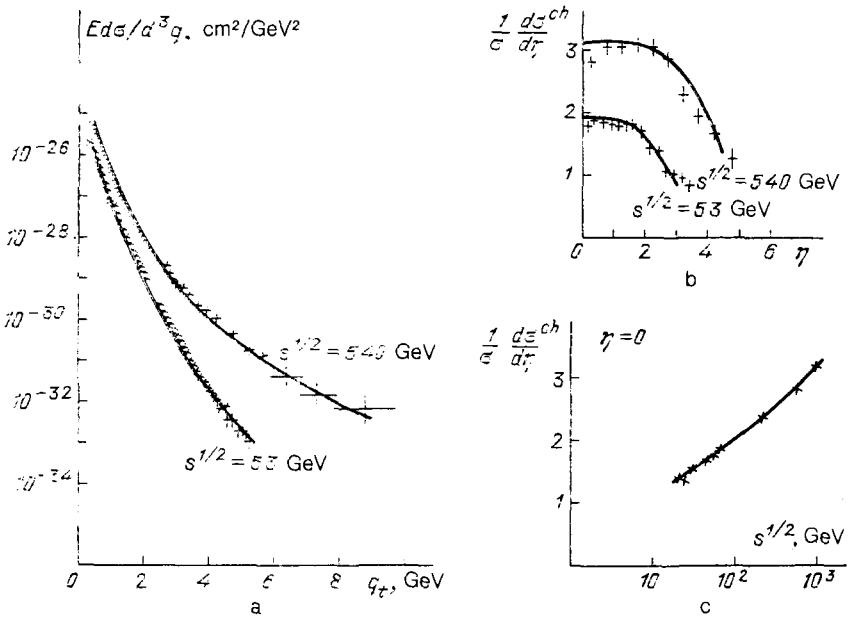

FIG. 10. Inclusive cross section for the production of secondary hadrons as a function of transverse momentum (for $y = 0$) (a), rapidity (b), and initial energy ($y = 0$) (c). The data are taken from Refs. 110–112.

to within 20–30% with estimates based on calculations using low-order QCD perturbation theory.

Although none of our calculations had anything in common with thermodynamics, the emerging picture is outwardly similar to the quark-gluon plasma (QGP). The rapid increase in the energy per unit volume, ε, is in accordance with the expression $\varepsilon \propto q_0^3/\tau_0 \propto \exp[3.8\ (\ln s)^{1/2}]$, and already for the SppS collider energy $s^{1/2} = 0.54$ TeV, we have $\varepsilon \approx 33$ GeV/fm². There is a corresponding increase in the effective temperature (average kinetic energy associated with the transverse motion of gluons), which reaches about 1 GeV for $s^{1/2} = 1$ TeV. Such high "temperatures" are associated with high relative yields of heavy particles (strangeness, charm), and since the number of collisions between partons with momenta $q_t < q_0$ is large, we have something close to an equilibrium distribution in transverse space. However, the system as a whole is not in equilibrium. First, the interaction cross sections of particles with $q_t > q_0$ are too small, so that they freely leave the system to form jets of hadrons with power-type "tails," i.e., their momentum distributions are $d\sigma/dq_t^2 \propto q_t^{-4}$ (for $q_t \gg q_0$). Second, there is no reason (and simply not enough time) for the establishment of equilibrium in the longitudinal momenta. Nevertheless, the strong fluctuations in multiplicity (number m of combs) and transverse momenta (due to diffusion in $\ln q_t$) that are typical for this scheme significantly impede the segregation of QGP. An event tentatively identified as a manifestation of QGP may turn out to be a fluctuation in the ordinary multiple production process. Even the increase in the mean $\langle q_t \rangle$ with multiplicity, which is often looked upon as an indication of a phase transition to the QGP state, has a different and perfectly obvious explanation in this scheme.

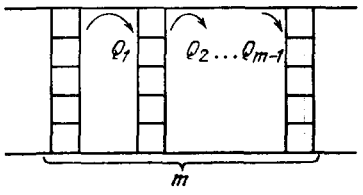

FIG. 11.

6.2. *Diffraction dissociation.* The main contribution to the dissociation cross section is provided by collisions with large impact parameters $b_t \gtrsim R(y)$ (Refs. 31, 32, and 81). It is only in such cases (when the parton density is low) that there is a sufficiently high probability that the interaction will not destroy completely the wave function of the initial fast hadron. Correspondingly, the cross section σ^D is proportional to the area of the edge of the disk $\sigma^D \propto \pi R/m_\pi \propto \ln s$, and increases with energy as the first power of its logarithm.

Graphically, this is seen as the screening of the contribution of the diagram of Fig. 14a by the unenhanced diagrams of Fig. 14b, so that the total contribution $M_{a+b} = M_a(1 + if(b,s))$ tends to zero in the interior of the black disk, where $f \to i$. This cancellation occurs everywhere except for the edge of the disk, where $|f| < 1$.

If we calculate the total dissociation cross section on the

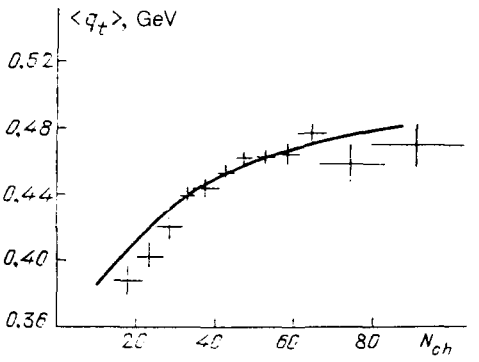

FIG. 12. Mean transverse momentum as a function of the multiplicity of charged hadrons in an event. The curve represents the calculation that takes into account diffusion in the space of $\ln Q_t$. The data are taken from Ref. 114; $s^{1/2} = 540$ GeV.

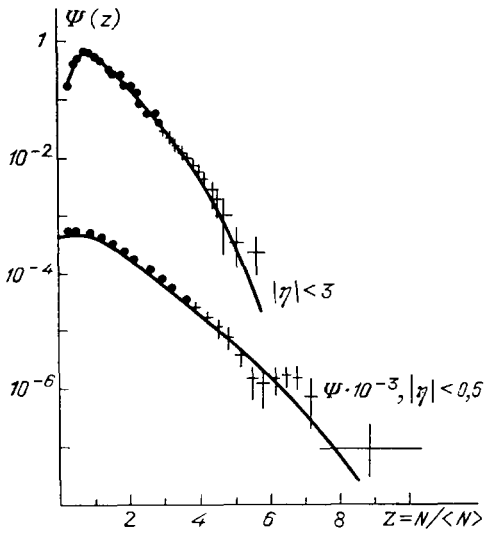

FIG. 13. Multiplicity distributions for charged hadrons. Data are taken from Ref. 115; $s^{1/2} = 540$ GeV, $\sigma_N = \sigma_{in}\Psi(z)/\langle N\rangle$.

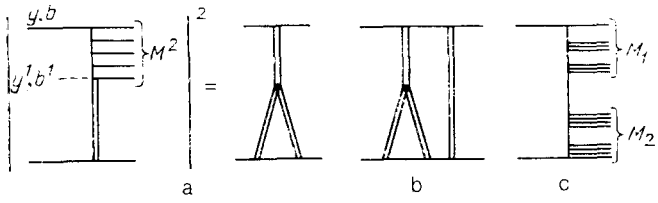

FIG. 14.

assumption that the interaction range R increases linearly as a function of the logarithm of the energy, $R = ay$, then, as already noted in Sec. 1.7(2), the integral with respect to the mass of the newly created state M^2 will diverge logarithmically,i.e.,

$$\sigma^D = \int dM^2\, d\frac{\sigma^D}{dM^2} = \int |1 + if(b, s)|^2 |^2 d^2b g \int |f(b', y')|^2 \times \operatorname{Im} f(b-b', y-y')\, d^2b'\, dy' \quad \left(dy' = \frac{dM^2}{M^2}\right), \quad (34)$$

which is similar to what happened to ordinary three-pomeron formulas ($d\sigma^{3P}/dM^2 \propto G_{3P}/M^2$, $\sigma^{3P} \propto \ln M^2$), and the probability of dissociation at the point b_t at the edge of the disk is found to be greater than the total probability of inelastic interaction $G_{in}(b_t)$ at this point. The contradiction is resolved by taking into account the nonlinear correction (7) in the expression for the range $R(y) = ay - \beta \ln y$ (Ref. 30). At this point, we shall already use the self-consistent value $\beta = 1/m_\pi$. Hence, in the significant region $b \gtrsim R(y)$, in which the function $f(b)$ falls as $\exp[(R(y) - b)/2m_\pi]$, the cross section is

$$\frac{d\sigma}{dM^2} = \int \frac{d^2b}{M^2} |1 + if(b, s)|^2 g |f(b', y')|^2 \times \operatorname{Im} f(b-b', y-y')\, d^2b' \propto \frac{2\pi R(y) 2m_\pi}{M^2 \{y'[1-(y'-y)]\}^{3/2}}$$

and the integral with respect to the masses $dM^2/M^2 = dy'$ is found to converge satisfactorily. The dissociation cross section $\sigma^D \propto \pi R(y)/m_\pi$ increases with energy more slowly than the total or elastic cross sections $\sigma_{el} \to \sigma_t/2 \approx \pi R^2$, and $\sigma^D/\sigma_{el} \to 0$ as $s \to \infty$. A similar convergence is found for the integrals of the differential cross sections for multi-reggeon (multi-froissarton) processes whose main contribution is concentrated in the region of finite masses M_1 and M_2 (see Fig. 14c). A further interesting difference, as compared with the old three-pomeron phenomenology, is that, whereas the previous inclusive distributions in the system M^2 produced by diffraction dissociation were found to be the same as the distributions in ordinary inelastic interactions for $s = M^2$, we now find that, in the case of dissociation on a froissarton, for which only the edge of the disk is significant, the transverse momenta of secondary particles $q_t \sim q_0(b', y') \sim Q_0$ [since $b' \geqslant R(y') \approx a \ln(1/x)$, see (32)] do not increase with increasing mass M^2 whereas, in inelastic processes, the characteristic momenta of gluon minijets $q_t \sim q_0(b', y')$ (for $b' \ll R(y')$) increase in accordance with the expression $\ln q_t \approx 1.26(\ln s)^{1/2}$.

7. CONCLUSION

The overall conclusion of our review is that the QCD perturbation theory is a good basis for an understanding of the interaction between high-energy hadrons, and this includes not only total and diffraction cross sections, but also inelastic processes such as the multiple production of secondary hadrons. As the energy increases, the cross section $\sigma_t \propto \ln^2 s$ and the interaction range $R \propto \ln s$ increase at a maximum rate. The increase in the interaction range is mostly due to the emission of gluons with $q_t \sim Q_0$ from the periphery of the disk, whereas blackening, i.e., the increase in the probability of interaction at a given point $b_t < R$, is due to the emission of gluon minijets with numerically large $q_t \sim q_0$. Correspondingly, the characteristic transverse momenta of minijets in ordinary inelastic processes increase with energy in accordance with the expression $q_t \sim q_0 \propto \exp[1.26(\ln s)^{1/2}]$, and the multiplicity is given by $N \propto q_0^2 \propto \exp[2.52(\ln s)^{1/2}]$.

The qualitative features of the dynamics of fast-hadron interactions that we have enumerated here correctly reflect the basic tendencies in the behavior of modern experimental data. The successful description of data, even by a relatively simple model, suggests that the interaction picture that we favor here will remain valid (as it develops) both qualitatively and quantitatively.

[1)] In the absence of theoretical ideas on the mechanism that could ensure the annulment of G_{3P} from the microscopic point of view.

[2)] At one time, Chou and Yang[17] used the model in which the amplitude for the scattering of two particles a and b was proportional to the product of their formfactors: $A(s,t) = icsG_a(t)G_b(t)$ (c = const). Correspondingly, the function $f(s,b)$ was a convolution of the density distributions $\rho(b)$:

$$f(s, \mathbf{b}) \propto \int \rho_a(\mathbf{b}')\rho_b(\mathbf{b} - \mathbf{b}')\, d^2b'.$$

[3)] It has been suggested in the literature that the UA1 data could be described, without introducing jets, as fluctuations in soft processes. The authors of the UA1 experiment do not agree with this idea. They estimate that only 18% of minijets with $p_t > 5$ GeV can be explained in terms of fluctuations in soft processes (see Sec. 6.1).

[4)] At high energies, each value of b_t corresponds to a particular partial wave $l \approx b_t s^{1/2}/2$, and the unitarity condition

$$2 \operatorname{Im} f(b, s) = |f(b, s)|^2 + G_{in}(b, s)$$

for amplitudes

$$f(b,\ s) = \int M(q_t s)\ e^{iqb}\ d^2q_t(8\pi^2 s)^{-1}$$

is equivalent to the usual unitarity condition for waves with given orbital momentum l.

[5)]The interaction picture described above and the mechanism responsible for screening are satisfactorily reproduced by (24), discussed in detail in Sec. 5.

[6)]More precisely: a point target parton (test particle) interacts with a gluon...

[7)]The quantity Q_0 is determined by the initial conditions, i.e., the structure of the incident hadron and the effect of the confinement mechanism.

[8)]We shall show later that the rescattering probability for the i-th parton in this type of chain is proportional to the constant $\alpha_s(q_{ti}) \ll 1$.

[9)]Of course, the effect of confinement is unrelated to diffusion in the space of $\ln q_t$ for numerically large q_t, where $\alpha_s(q_t) \ll 1$. Confinement merely limits diffusion to very small q_t for which the gluon wavelength $\lambda \sim 1/q_t$ is comparable with the hadron radius $\langle r \rangle \sim 1$ fm.

[10)]For example, when $y_1 = y/2$, we have $\ln y_1 + \ln(y - y_1) = 2\ln(y/2) = 2\ln y - 2\ln 2 > \ln y$.

[11)]For $s^{1/2} > 1$ TeV, the cross sections were obtained in a somewhat indirect manner. In practice, the distributions were measured by determining the height of the point at which an extensive atmospheric shower (EAS) was produced. Taking this as a starting point, a calculation was made of the cross sections for the interaction between the incident proton and an air nucleus (mostly ^{14}N), and the next step was to calculate the nucleon-nucleon scattering cross section in the Glauber approximation. A more detailed discussion of cosmic-ray data can be found in Ref. 45.

[12)]In the case of strong coupling, $R = \ln^{\eta} s$, where $\eta \geqslant \beta/2$.

[13)]There are reasons to suppose that the estimate $\sigma_{in}(p - \text{Air}) = 540 \pm 50$ mb is too high. When the increase in the inelasticity coefficient is taken into account, the more probable result is found to be $\sigma_{in}(p - \text{Air}) = 450 \pm 50$ mb. The slope $B_{NN} \approx 20$ GeV^{-2} is then much greater than $\alpha'(s^{1/2} = 10\text{–}50\ \text{GeV}) = 0.12 \pm 0.03$ GeV^{-2}. As can be seen, despite the considerable uncertainties in cosmic-ray data, the qualitative conclusions based upon them remain valid.

[14)]This approximation has been fully confirmed experimentally for small t for which the amplitude with spin flip is small ($\lesssim t^{1/2}/2m_N$), and the spin–spin correlations decrease with energy at least as $1/\ln^6 s$ (Ref. 6).

[15)]The distributions over the transverse momenta, $d\sigma/dp_t$, depend entirely on the assumptions made about the internal structure of the reggeon itself (the vertex for the emission of a hadron by the reggeon) and are not critical in such models. As a rule, the transverse momentum spectra of the particles are not as well described as the longitudinal spectra.

[16)]As a rule, only the simplest two-particle unitarization [see (19)] is taken into account.

[17)]It is important to emphasize that, although the authors of Ref. 88 used formulas resembling the expressions for the inclusive cross sections, only a part of the total cross section was actually calculated. The point is that the range of integration with respect to the fraction x of the parton momentum was artificially restricted by the condition $x > m^2/|t|$. (Of course, this type of limitation was incorrect, but these authors were concerned only with part of the total cross section.) As a result, the intervals of variation of x in blocks that describe the structure functions of the colliding hadrons and in the hard scattering block with the transfer of the square of momentum t, do not intersect and there is no double counting.

[18)]In this context, it is not entirely clear what is the parton–parton cross section, but a detailed study of the structure of the parton cascade[99] shows that, in the language of Feynman diagrams, the inequality $\tilde{\sigma} < \ln^2 \hat{s}$ remains valid.

[19)]If we accept the analogy with scattering by the nucleus, the internal transverse momentum is defined as being of the order of the reciprocal of the size of a nucleon ($p_t \sim 300$ MeV) that is typical for each individual nucleon-nucleon interaction (parton-parton in our case) and is not the size of the nucleus ($p_t \sim 1/R_A \propto A^{-1/3}$) that characterizes, for example, the width of the diffraction cone in elastic collisions or diffraction dissociation on the nucleus.

[20)]The other argument for the simultaneous introduction of coordinates q_t and b_t is that, during iteration of (24), the soft parton (gluon) acquires its own values of the coordinate and transverse momentum at different stages of development (different "times" $it = y$). Displacement in the plane of impact parameters occurs in those cells of the ladder in which the transverse momentum q_i' is small (since $\Delta b_t \propto 1/q_i'$), and the final q_t accumulates due to cells (iterations) with large q_i'. Hence, after integration with respect to the momenta of intermediate gluons (in the inclusive formulation of the problem), the coordinates q_t and b_t are unrelated.

[21)]Unfortunately, this fact, i.e., the increase in q_t as a result of rescattering, is not included in the simplified expression given by (24), and the integration range is restricted to small q_i' in a somewhat crude manner [see below, (32)]. This means that when we solve (24), we must introduce an additional boundary condition of the form $\varphi(x,q) \to 0$ for some fixed and numerically large $q \to \bar{Q}_0$, and consider (24) only for $q > \bar{Q}_0(\alpha_s(\bar{Q}_0) < 1)$ for which the confinement mechanism is still relatively unimportant. The conditions

$$\varphi \to 0$$

or

$$\frac{\partial \varphi}{\partial q^2}\bigg|_{q=\bar{Q}_0} \to 0$$

guarantee the absence of a flux of new partons from the region of small $q_t < \bar{Q}_0$ (in which the effect of confinement can manifest itself) and have practically no effect on the form of the solution for $q_t \geqslant q_0(x)$ with $q_0(x, b_t) \gg \bar{Q}_0$.

[22)]Concrete estimates made in QCD perturbation theory show that the average number of diffusion steps in the gluon cascade for which $\varphi = \varphi_0$ is reached is $\langle n \rangle \approx 1.7$. The transverse momentum increases by a factor of 5 during this diffusion, i.e., $Q_0 \approx 5q_{in}$.

[1]M. Baker and K. A. Ter-Martirosyan, Phys. Rep. **28**, 1 (1976); P. D. B. Collins, An Introduction to Regge Theory and High-energy Physics, Cambridge Univ. Press, Cambridge, 1971. [Russ. transl., Atomizdat, M., 1980].

[2]V. N. Gribov and A. A. Migdal, Yad. Fiz. **8**, 1002 (1968) [Sov. J. Nucl. Phys. **8**, 583 (1969)].

[3]H. D. I. Abarbanel, V. N. Gribov, and O. V. Kancheli, FNAL Preprint, THY-76, August 1972.

[4]A. B. Kaĭdalov, Phys. Rep. **50**, 157 (1979).

[5]D. R. Roy and R. G. Roberts, Nuclear Physics B **77**, 240 (1974).

[6]Ya. I. Azimov *et al.*, Proc. Ninth Winter School of the Leningrad Nuclear Physics Institute, Academy of Sciences of the USSR **2**, 5 (1974). (In Russian).

[7]D. Amati, S. Fubini, and A. Stanghelini, Nuovo Cimento **26**, 896 (1962).

[8]E. L. Feinberg and D. S. Chernavskiĭ, Usp. Fiz. Nauk **82**, 3 (1964) [Sov. Phys.—Usp. **7**, 1 (1964)].

[9]E. M. Volkov, I. M. Dremin, A. M. Dunaevskiĭ, I. I. Roĭzen, and Chernavskiĭ, Yad. Fiz. **17**, 407 (1973) [Sov. J. Nucl. Phys. **17**, 208 (1973)].

[10]K. G. Boreskov, A. B. Kaĭdalov, and L. A. Ponomarev, ITEF-950 Preprint, Moscow, 1972 (In Russian).

[11]E. M. Levin and M. G. Ryskin, Yad. Fiz. **17**, 388 (1973) [Sov. J. Nucl. Phys. **17**, 199 (1973)].

[12]V. N. Gribov and A. A. Migdal, Zh. Eksp. Teor. Fiz. **55**, 1498 (1968) [Sov. Phys.—JETP **28**, 784 (1969)].

[13]V. N. Gribov, Zh. Eksp. Teor. Fiz. **53**, 654 (1967) [Sov. Phys.—JETP **26**, 414 (1968)].

[14]V. A. Abramovskiĭ, V. N. Gribov, and O. V. Kancheli, Yad. Fiz. **18**, 595 (1973) [Sov. J. Nucl. Phys. **18**, 308 (1973)].

[15]H. D. I. Abarbanel, J. B. Bronzan, *et al.*, Phys. Rep. **21** C, 119 (1975).

[16]M. Moshe, *ibid.* **37** C, 255 (1978).

[17]T. T. Chou and C. N. Yang, Phys. Rev. **170**, 1591 (1968); Phys. Lett. B **128**, 457.

[18]K. Hanzi and P. Valin, *ibid.* **160**, 167 (1985).

[19]F. Ceradini, Preprint CERN-EP/86-142, Geneva, 1986.

[20]G. Pancheri and Y. N. Srivastava, Preprint, Harvard University, HUTP-86/A061, Cambridge, Mass., 1986.

[21]V. N. Gribov, Yad. Fiz. **9**, 640 (1969) [Sov. J. Nucl. Phys. **9**, 369 (1969)].

[22]M. G. Ryskin, Proc. Seventh Winter School of the Leningrad Inst. Nucl. Phys. **1**, 131 (1972). (In Russian).

[23]M. Froissart, Phys. Rev. **123**, 1053 (1961).

[24]A. A. Migdal, A. M. Polyakov, and K. A. Ter-Martirosyan, Zh. Eksp. Teor. Fiz. **67**, 848 (1974) [Sov. Phys.—JETP **40**, 420 (1975)]; H. D. I. Abarbanel and J. B. Bronzan, Phys. Lett. B **48**, 345 (1974); Phys. Rev. D **9**, 2397 (1974).

[25]M. Baig, J. Bartels, and J. W. Dash, Nucl. Phys. B**237**, 502 (1984).

[26]J. N. Dash and S. I. Jones, Phys. Rev. D **33**, 1512 (1986).

[27]Sh. S. Eremyan and V. M. Zhamkochyan, Yad. Fiz. **40**, 1016 (1984) [Sov. J. Nucl. Phys. **40**, 648 (1984)].

[28]E. A. Kuraev, L. N. Lipatov, and V. S. Fadin, Zh. Eksp. Teor. Fiz. **72**, 377 (1977) [Sov. Phys.—JETP **45**, 199 (1977)].

[29]M. S. Dubovikov and K. A. Ter-Martirosyan, Nucl. Phys. B **124**, 163 (1977).

[30]E. M. Levin and M. G. Ryskin, Preprint, Leningrad Inst. Nucl. Phys., No. 370, 1977 (In Russian); M. G. Ryskin, *ibid.* No. 1419, 1988. (In Russian).

[31]J. L. Cardy, Nucl. Phys. B **75**, 413 (1974).

[32]G. Marchesini and E. Rabinovici, *ibid.* **120**, 253 (1977).
[33]E. M. Levin and M. G. Ryskin, Yad. Fiz. **25**, 849 (1977) [Sov. J. Nucl. Phys. **25**, 452 (1977)].
[34]K. A. Ter-Martirosyan, Zh. Eksp. Teor. Fiz. **44**, 341 (1963) [Sov. Phys.—JETP **17**, 233 (1963)]; I. A. Verdiev, O. V. Kancheli, S. G. Matinyan, A. M. Popova, and K. A. Ter-Martirosyan, Zh. Eksp. Teor. Fiz. **46**, 1700 (1964) [Sov. Phys.—JETP **19**, 1148 (1964)].
[35]J. Finkelstein and K. Kajantie, Phys. Lett. **B26**, 305 (1968).
[36]Yu. P. Gorin *et al.*, Yad. Fiz. **14**, 998 (1971) [Sov. J. Nucl. Phys. **14**, 560 (1975)].
[37]A. I. Lendel and K. A. Ter-Martirosyan, Pis'ma Zh. Eksp. Teor. Fiz. **11**, 70 (1970) [JETP Lett. **11**, 45 (1970)]; K. G. Boreskov, A. M. Lapidus, S. T. Sukhorukov, and K. A. Ter-Martirosyan, Yad. Fiz. **14**, 814 (1971) [Sov. J. Nucl. Phys. **14**, 457 (1972)].
[38]A. V. Amaldi *et al.*, Phys. Lett. **44**, 118 (1973).
[39]A. S. Caroll *et al.*, Phys. Rev. Lett. **33**, 298 (1974).
[40]A. N. Diddens *et al.*, Proc. Seventeenth Int. Conf. On High Energy Physics, London, 1974, p. 1.
[41]G. Arnison *et al.*, Phys. Lett. **B128**, 336 (1983); M. Bozzo *et al.*, *ibid.*, **147**, 392 and 385 (1984).
[42]G. J. Alner *et al.*, Z. Phys. **C32**, 153 (1986).
[43]T. Hara *et al.*, Phys. Rev. Lett. **50**, 2058 (1983).
[44]R. M. Baltrusaitis *et al.*, *ibid.* **52**, 1380 (1984).
[45]T. Hara *et al.*, Proc. Int. Symp. on Cosmic Rays and Particle Physics, Tokyo, 1984; R. M. Baltrusaitis *et al.*, Proc. Nineteenth Cosmic Ray Conf., La Jolla, 1985 **6**, p. 5.
[46]G. B Yodh, Y. Pal, and J. S. Frelil, Phys. Rev. Lett. **28**, 1005 (1972).
[47]A. O. Barut and S. Boukraa, Preprint IC/87/83, Trieste, 1987.
[48]M. M. Block and R. N. Cahn, Phys. Lett. **B188**, 143 (1987).
[49]K. M. Chernev *et al. ibid.*, **36**, 266 (1971).
[50]V. D. Bartenev *et al.*, Phys. Rev. Lett. **39**, 1088 (1973); L. A. Fajardo *et al.*, Phys. Rev. **D24**, 46 (1981).
[51]V. Amaldi *et al.*, Phys. Lett. **B66**, 390 (1977).
[52]L. Baksay *et al.*, Nucl. Phys. **B141**, 1 (1978).
[53]J. P. Burg *et al.*, Phys. Lett. **B109**, 124 (1982).
[54]J. P. Burg *et al.*, Phys. Lett. B, Nucl. Phys. **B217**, 285 (1983).
[55]Sh. S. Eremyan and V. M. Zhamkochyan, Vopr. at. nauki i tekh., Ser. TFE **17** (29), 3 (1986).
[56]B. Z. Kopeliovich, N. N. Nikolaev, and I. K. Potashnikova, Preprint, JINR-E2-86-125, Dubna, 1986.
[57]D. Bernard *et al.*, Phys. Lett. **B198**, 583 (1987).
[58]I. M. Dremin, Usp. Fiz. Nauk **155**, 139 (1988). [Sov. Phys. Usp. **31**, 462 (1988)].
[59]F. S. Henyey, R. Hong Tuan, and G. L. Kane, Nucl. Phys. B70, 445 (1974).
[60]A. B. Kaĭdalov, Yad. Fiz. **16**, 389 (1972) [Sov. J. Nucl. Phys. **16**, 217 (1972)].
[61]T. T. Chou and C. N. Yang **19**, 3268 (1979); A. J. Buras and J. Dias de Deus, Nucl. Phys. B**71**, 481 (1974).
[62]A. B. Kaĭdalov, Phys. Rev. Lett. B **116**, 459 (1982); A. B. Kaĭdalov and A. K. Ter-Martirosyan, Yad. Fiz. **39**, 1545 (1984) [Sov. J. Nucl. Phys. **39**, 979 (1984)]; A.B. Kaĭdalov and O. I. Piskunova, Yad. Fiz. **41**, 1278 (1985) [Sov. J. Nucl. Phys. **41**, 816 (1985)].
[63]A. Capella *et al.*, Phys. Lett. **B16**, 68 (1979); Z. Phys. C **3**, 329 (1980); Phys. Rev. **D32**, 2933 (1985).
[64]G. L. Kane and A. Seidl, Rev. Mod. Phys. **48**, 309 (1976).
[65]J. Pumplin and G. L. Kane, Phys. Rev. **D11**, 1183 (1975).
[66]L. D. Solov'ev, Pis'ma Zh. Eksp. Teor. Fiz. **18**, 455 (1973) [JETP Lett. **18**, 268 (1973)]; L. D. Solov'ev and A. V. Shchelkachev, Yad. Fiz. **42**, 984 (1985) [Sov. J. Nucl. Phys. **42**, 624 (1985)].
[67]S. M. Troshin and N. E. Tyurin, Yad. Fiz. **40**, 1008 (1984). [Sov. J. Nucl. Phys. **40**, 643 (1984)].
[68]L. L. Jenkovszky and A. N. Wall, Czech. J. Phys. **B26**, 447 (1976); A. N. Wall, L. L. Jenkovszky, and B. V. Struminskiĭ, Preprint, ITF-85-51R, Kiev, 1985. (In Russian).
[69]L. L. Jenkovszky, B. V. Struminskiĭ, and A. N. Shelkovenko, Preprint, ITF-86-105R, Kiev, 1986. (In Russian).
[70]A. Donnachie and P. V. Landshoff, Phys. Lett. **B123**, 345 (1983); Nucl. Phys. **B244**, 322 (1986); *ibid.* **267**, 690 (1986).
[71]P. Gauron, B. Nicolescu, and E. Leader, Phys. Rev. Lett. **54**, 2656 (1985).
[72]A. G. Bourelli, J. Soffer, and T. T. Wu, *ibid.* **54**, 757 (1985).
[73]J. W. Dash, S. T. Jones, and E. K. Menesis, Phys. Rev. D **18**, 303 (1978); J. W. Dash and S. T. Jones, Phys. Lett B **157**, 229 (1985); Preprint, UA HEP-869/CPT-87/PE, Alabama, 1986.
[74]A. Bohm *et al.* Phys. Lett. **B49**, 491 (1974); S. Erhan *et al.* **152**, 131 (1985).
[75]M. Bozo *et al.*, *ibid.* **155**, 197 (1985); D. Bernard, *et al.*, *ibid.* **171**, 142 (1986).
[76]S. S. Gershteĭn and A. A. Logunov, Yad. Fiz. **44**, 1251 (1986) [Sov. J. Nucl. Phys. **44**, 813 (1986)].
[77]C. L. Kane and Yorn Reng Yoo, Nucl. Phys. **B137**, 313 (1978).
[78]A. V. Kiselev and V. A. Petrov, Preprint, ITEV 85-180, Serpukhov, 1985. (In Russian).
[79]Yu. L. Dokshitzer, Zh. Eksp. Teor. Fiz. **73**, 1216 (1977) [Sov. Phys.—JETP **46**, 641 (1977)].
[80]G. Altarelli and G. Parisi, Nucl. Phys. **B126**, 296 (1977).
[81]A. B. Kaĭdalov, L. A. Ponomarev, and K. A. Ter-Martirosyan, Yad. Fiz. **44**, 722 (1986) [Sov. J. Nucl. Phys. **44**, 468 (1986)].
[82]T. K. Geisser and C.-I. Tan, Phys. Rev. **D8**, 3881 (1973); D. Sivers and F. von Hippel, *ibid.* **9**, 830 (1973); M. Suzuki, Nucl./ Phys. **B64**, 486 (1973); J. Koplik, *ibid.* **82**, 93 (1974).
[83]S. S. Gershteĭn and A. A. Logunov, Yad. Fiz. **39**, 1514 (1984) [Sov. J. Nucl. Phys. **39**, 960 (1984)].
[84]I. M. Dremin, Fiz. Elem. Chastits. At. Yadra **6**, 60 (1975) (sic.). A. B. Kaĭdalov, Elementary Particles [in Russian], Second Physics School, ITEF, M., 1975 **3**, p. 5.
[85]A. Kernan and G. van Dalen, Phys. Rep. **106**, 297 (1984); P. Weilhammer, Proc. Int. Symp. on Multiparticle Dynamics, Tashkent, 1987, World Scientific, Singapore, 1988, p. 711.
[86]D. Cline, F. Halzen, and J. Luthe, Phys. Rev. Lett. **31**, 491 (1973); S. D. Ellis and M. B. Kislinger, Phys. Rev. **D9**, 2027 (1974).
[87]F. Halzen, Nucl. Phys. **B92**, 404 (1975); T. K. Geisser and F. Halzen, Phys. Rev. Lett. **54**, 1754 (1985).
[88]G. Cohen-Tannoudji, A. Mantrach, H. Navelet, and R. Peschanski, Phys. Rev. **D28**, 1628 (1983).
[89]H. Navelet and R. Peschanski, Preprint, Saclay, SPhT-85-102, Paris, 1985.
[90]D. W. Tow, Phys. Rev. D **2**, 154 (1970).
[91]I. M. Dremin, I. I. Roĭzen, and D. S. Chernavskiĭ, Usp. Fiz. Nauk **101**, 385 (1970) [Sov. Phys. Usp. **13**, 438 (1971)].
[92]B. Webber, Phys. Rev. Lett. **27**, 448 (1971).
[93]L. Durand and P. Hong, *ibid.* **58**, 303 (1987).
[94]J. Kwiecinski, Phys. Lett. B **184**, 386 (1987); A. Capella, J. van Tran Thanh, and J. Kwiecinski, Phys. Rev. Lett. **58**, 2015 (1987).
[95]H. Cheng and T. T. Wu, *ibid.* **24**, 1456 (1970); Phys. Rev. **182**, 1852 (1969); *ibid.* D **1**, 2775 (1970).
[96]V. A. Abramovskiĭ, E. V. Gedalin, E. G. Gurvich, and O. V. Kancheli, Inelastic Interactions at High Energies and Chromodynamics [in Russian], Metsniereba, Tbilisi, 1986, p.112.
[97]A. A. Anselm and V. N. Gribov, Phys. Lett. **B40**, 487 (1972).
[98]L.V. Gribov *et al.*, Zh. Eksp. Teor. Fiz. **80**, 2132 (1981) [Sov. Phys.—JETP **53**, 1113 (1981)].
[99]L. V. Gribov *et al.*, Phys. Rep. **100**, 1 (1983).
[100]L. V. Gribov *et al.*, Yad. Fiz. **35**, 1278 (1982) [Sov. J. Nucl. Phys. **35**, 749 (1982)].
[101]D. Amati, L. Caneschi, and R. Jengo, Nucl. Phys. **B101**, 397 (1975); V. Alessandrini, D. Amati, and R. Jengo, *ibid.* **108**, 425 (1976); R. Jengo, *ibid.* p. 447.
[102]D. Amati, M. LeBellac, G. Marchesini, and M. Giafaloni, *ibid.* **112**, 107 (1976); D. Amati, M. LeBellac, G. Marchesini, and G. Parisi, *ibid.* **114**, 483 (1976).
[103]V. N. Gribov, Proc. Tenth Winter School [in Russian], Leningrad Inst. Nucl. Phys., Leningrad **1**, 5 (1975).
[104]E. M. Levin and M. G. Ryskin, Preprint, Leningrad Inst. Nucl. Phys., No. 1316, Leningrad, 1987. (In Russian).
[105]E. M. Levin and M. G. Ryskin, Yad. Fiz. **31**, 429 (1980) [Sov. J. Nucl. Phys. **31**, 226 (1980)].
[106]T.-S. Meng, see Ref. 85b, p. 543.
[107]C. Albajar *et al.*, CERN-AU1/DRAFT, August 11, 1987; Z. Phys. C, p. 140 (1987).
[108]B. I. Ermolaev and V. S. Fadin, Pis'ma Zh. Eksp. Teor. Fiz. **33**, 285 (1981) [JETP Lett. **33**, 269 (1981)]; V. S. Fadin, Yad. Fiz. **37**, 408 (1983) [Sov. J. Nucl. Phys. **37**, 245 (1983)]; A. H. Mueller, Proc. Int. Symp. on Lepton and Photon Interactions, Bonn, 1981 and Phys. Lett. **B104**, 161 (1981); A. Basseto, M. Giafaloni, G. Marchesini, and A. H. Mueller, Nucl. Phys. **B207**, 189 (1982); A. Basseto, M. Giafaloni, and G. Marchesini, Phys. Rep. **100**, 201 (1983); Ya. I. Azimov, Yu. L. Dokshitser, S. I. Troyan, and V. A. Khoze, Physics of Elementary Particles [in Russian], Proc. Twentieth Winter School, Leningrad Inst. Nucl. Phys., Leningrad, 1985, p. 82.
[109]M. G. Ryskin, Yad. Fiz. **47**, 230 (1988) [Sov. J. Nucl. Phys. **47**, 147 (1988)].
[110]G. Arnison *et al.*, Phys. Lett. **B118**, 167 (1982).
[111]K. Alpgard *et al.*, *ibid.* **107**, 310 (1981).
[112]J. Rushbrook *et al.*, Preprint, CERN-EP/85-124, Geneva, 1985.
[113]J. J. Aubert *et al.*, Nucl. Phys. **B272**, 58 (1986).
[114]A. DiCiaccio, Proc. Seventeenth Symp. Multiparticle Dynamics, Seewinkel, June, 1986.
[115]G. J. Alner *et al.*, Phys. Lett. **B160**, 193 (1985).

Translated by S. Chomet